IAEA Technical Meeting on Atomic, Molecular and Plasma-Material Interaction Data Evaluation and Development

Experimental potentials for atomic data for fusion research and astrophysics at Lanzhou

Xinwen Ma

Institute of Modern Physics, Chinese Academy of Sciences

2018.11.19-21, IAEA, Vienna, Austria

Motivation

HCI: Astrophysical plasma and Fusion Plasma

Collisionally ionized plasma formed in stars, supernova remnants, and galaxies

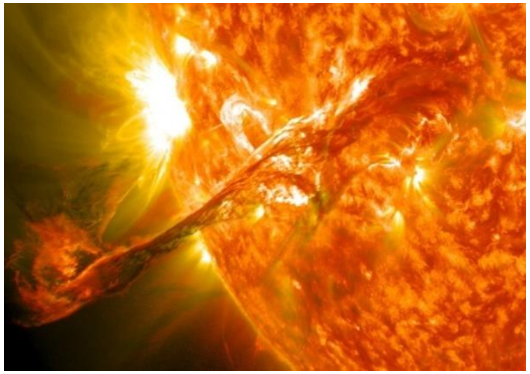
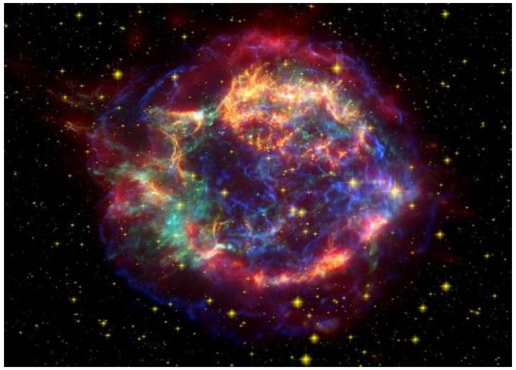


photoionized plasmas formed in planetary nebulae, X-ray binaries, and AGN

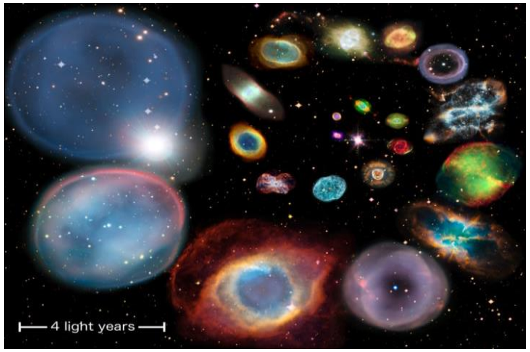

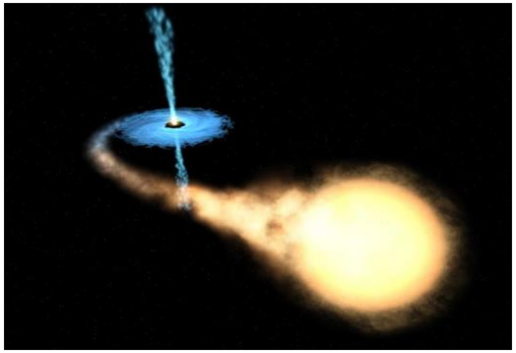


1. Experimental facilities for atomic ions/molecular ions collisions.

2. Some typical results related to the atomic data for fusion research and astrophysics.

3. Near future working plans and collective action of data for fusion research and astrophysics.

Experiments of HCIs @ Lanzhou

Heavy Ion Research Facility in Lanzhou (HIRFL)

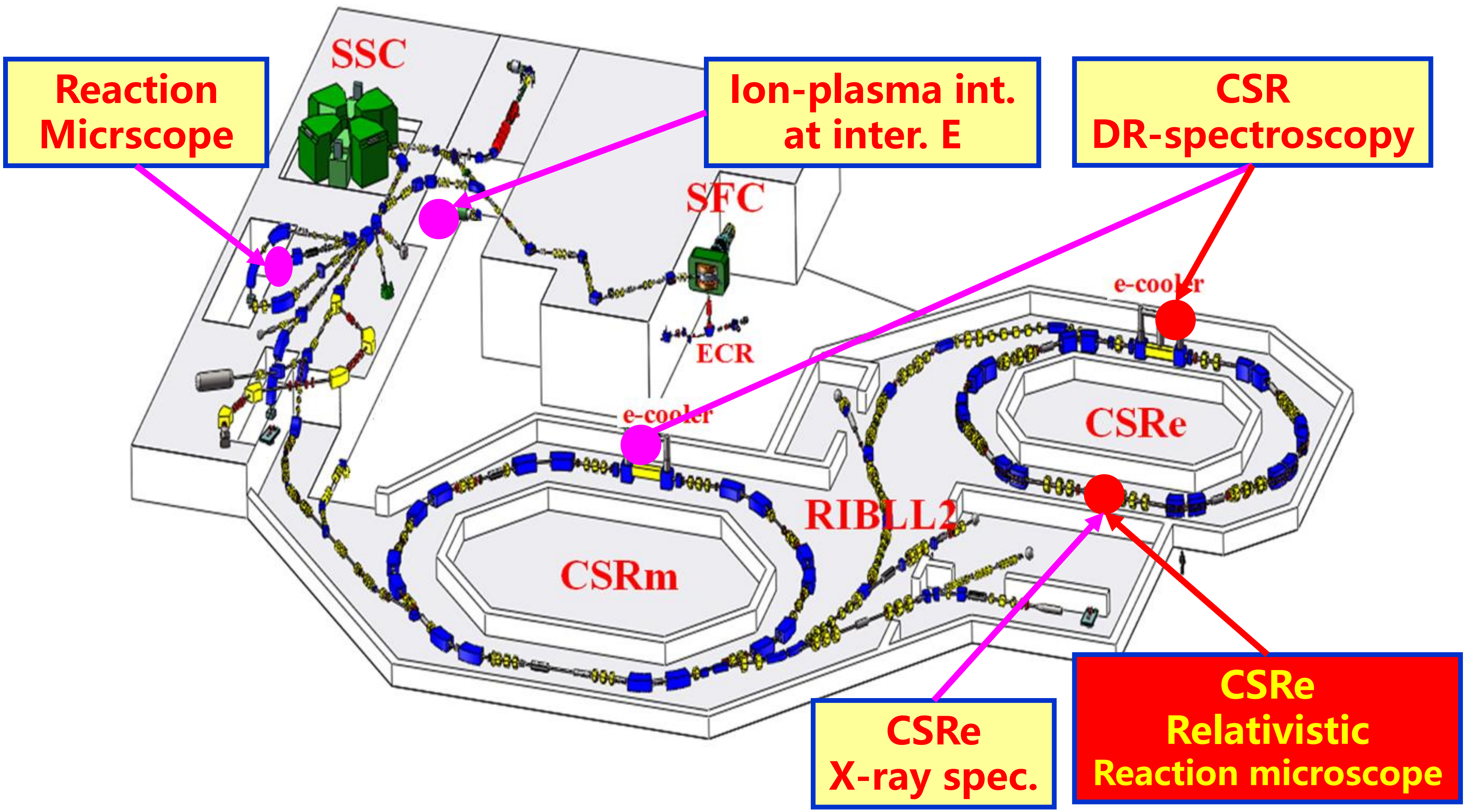

Experiments of HCIs @ Lanzhou

320 kV Platform for multi-disciplinary research with HCIs

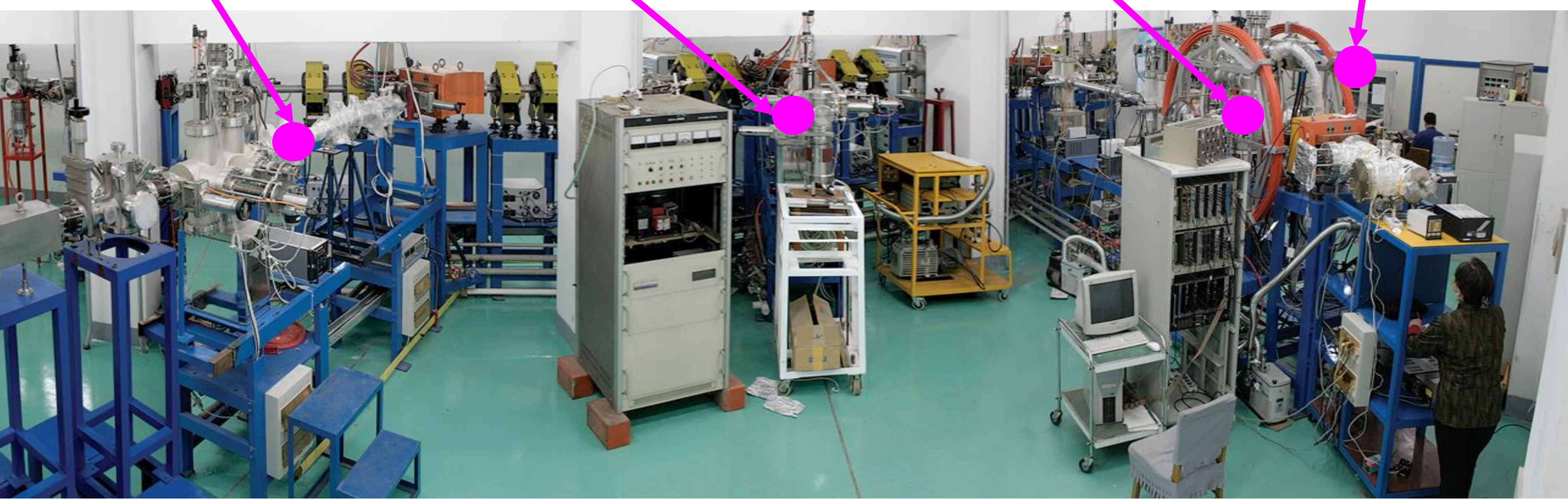

Experiments of HCIs @ Lanzhou

320kV platform for Multi-disciplinary Research with HCIs

Ion-plasma interaction

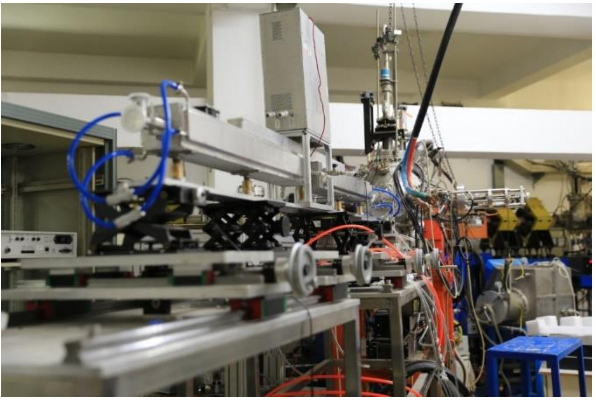

Reaction microscope

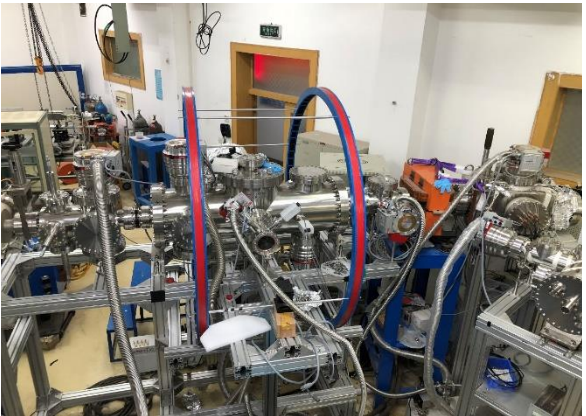

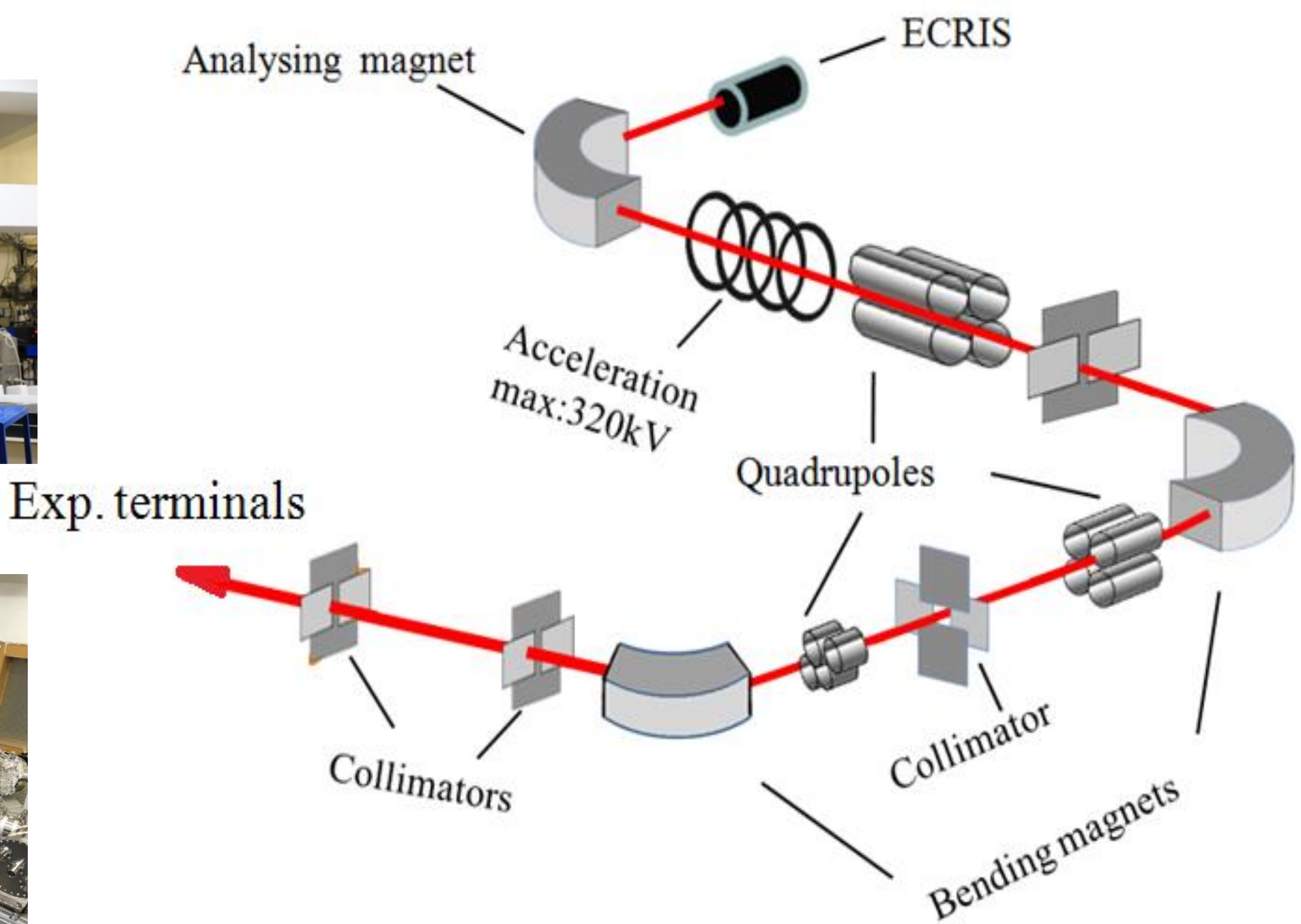

Experiments of HCIs @ Lanzhou

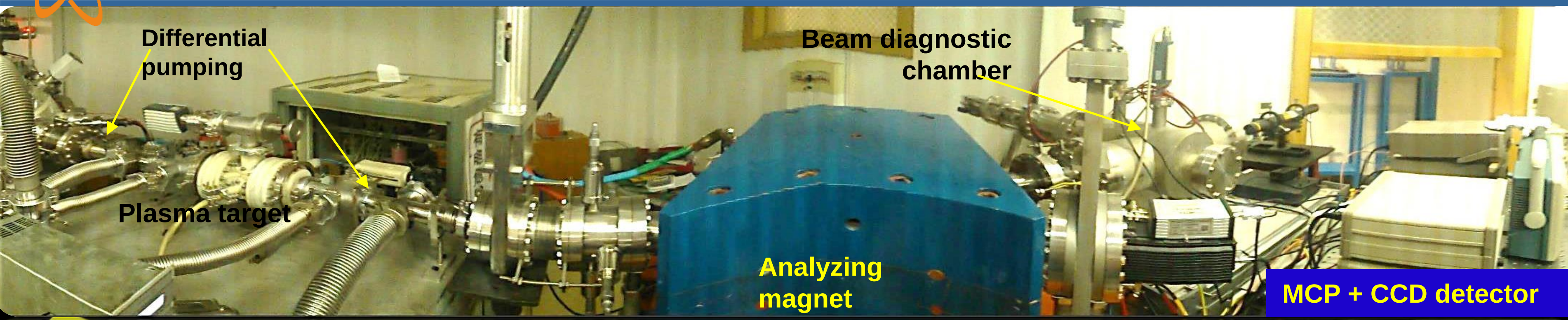

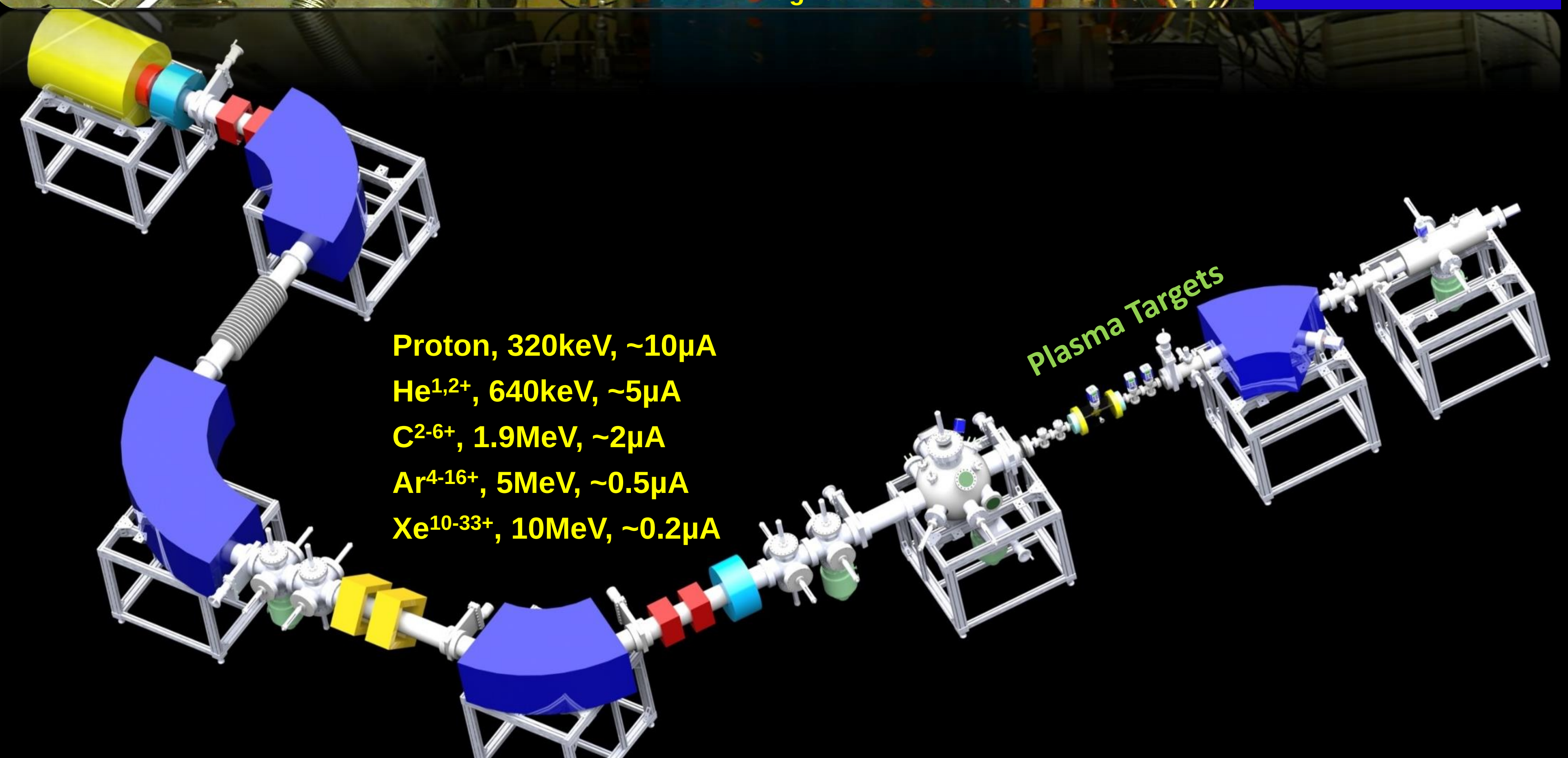

Proton, 320keV, ~10μA

$He^{1,2+}$, 640keV, ~5μA

$C^{2\text{-}6+}$, 1.9MeV, ~2μA

$Ar^{4\text{-}16+}$, 5MeV, ~0.5μA

$Xe^{10\text{-}33+}$, 10MeV, ~0.2μA

Experiments of HCIs @ Lanzhou

Very-low energy platform: EBIS-A facility

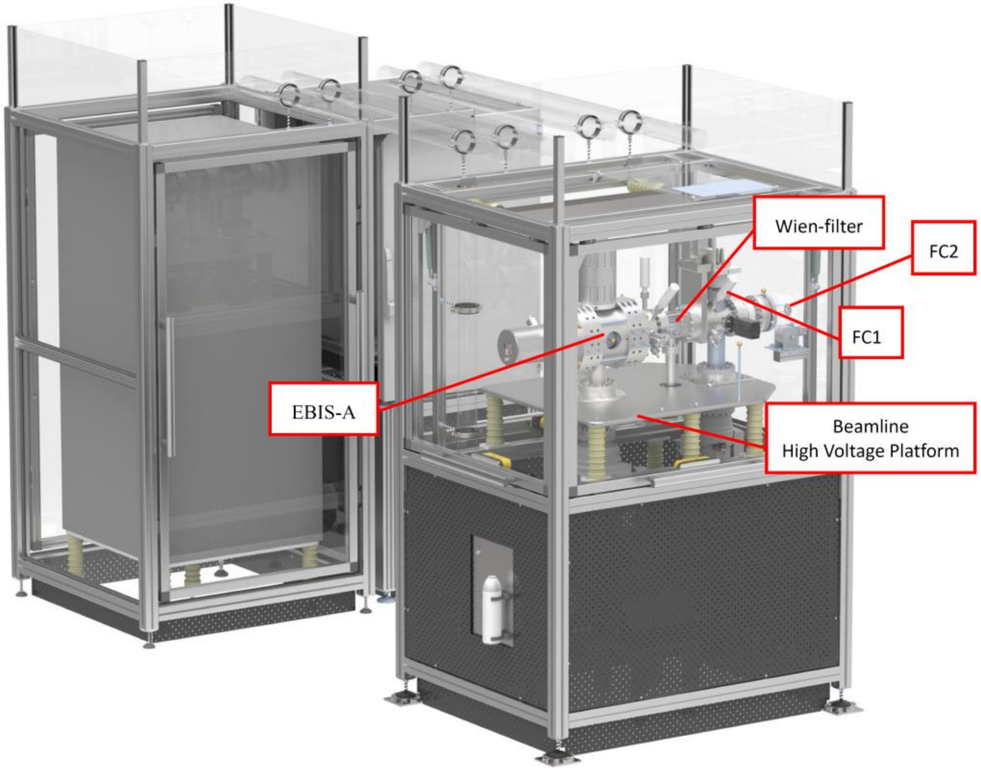

Dresden EBIS-A ion source

Kinetic Energy: 500 q eV – 30 q keV

COTRIMS for
Charge Exchange Experiments

Experiments of HCIs @ Lanzhou

C icroscopy @ EBIS

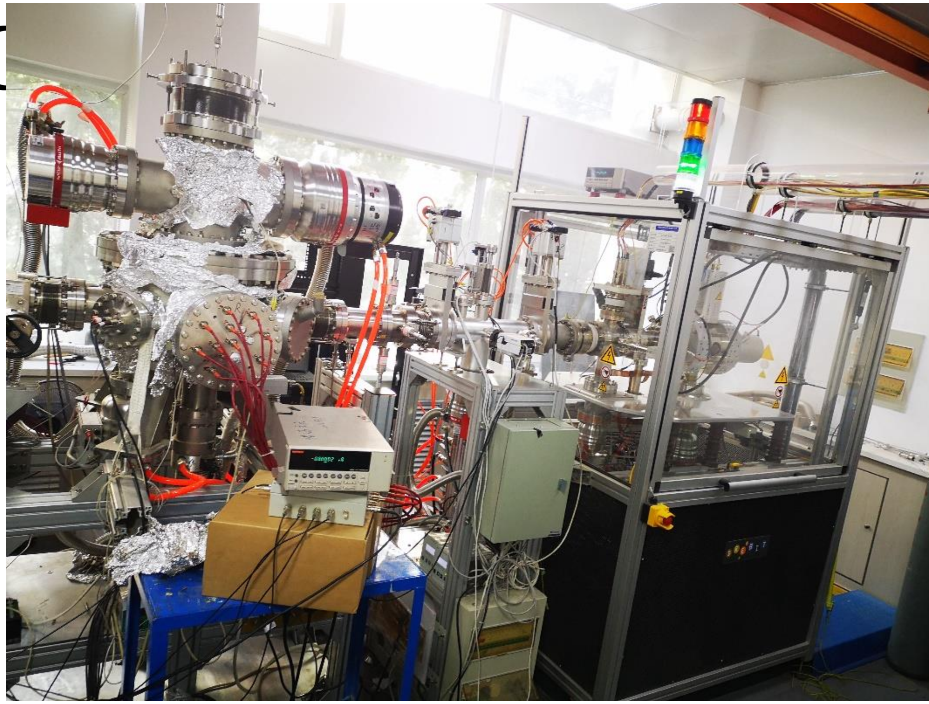

Electron capture:

$$P_{long} = -\frac{\boldsymbol{Q}}{v_p} - \frac{1}{2} \cdot n_c \cdot v_p$$

$$P_{trans} = p_0 \cdot \boldsymbol{\theta}$$

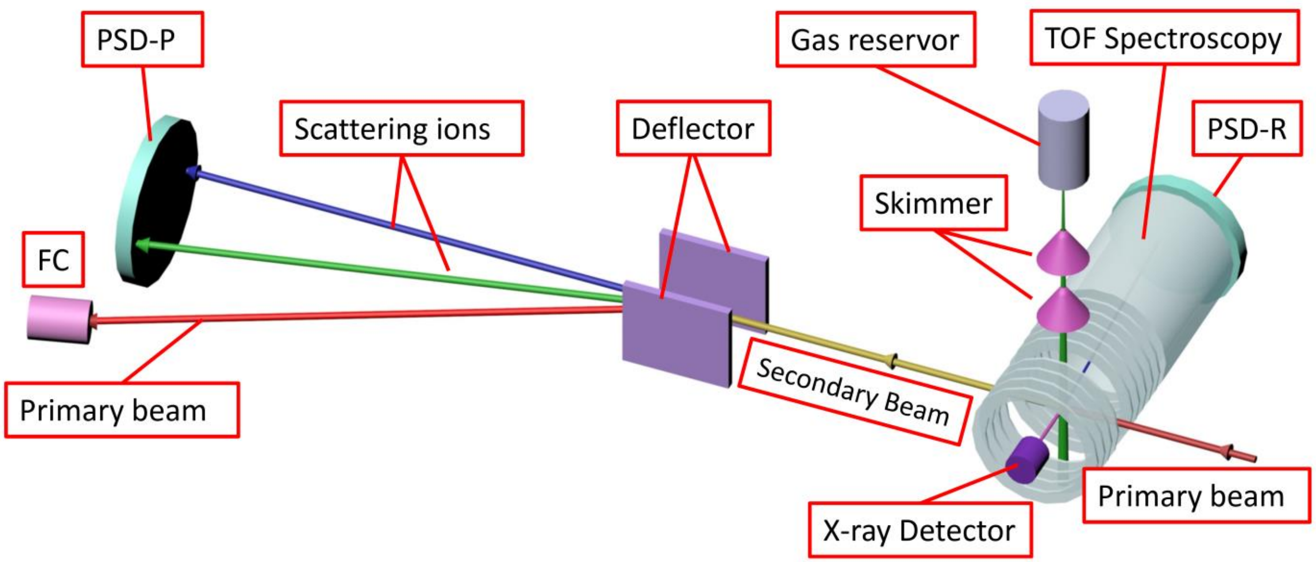

2. Some typical results related to the atomic data for fusion research and astrophysics

2.1 Charge exchange processes

State-resolved SEC in Ar^{8+}-He @ 3keV/u

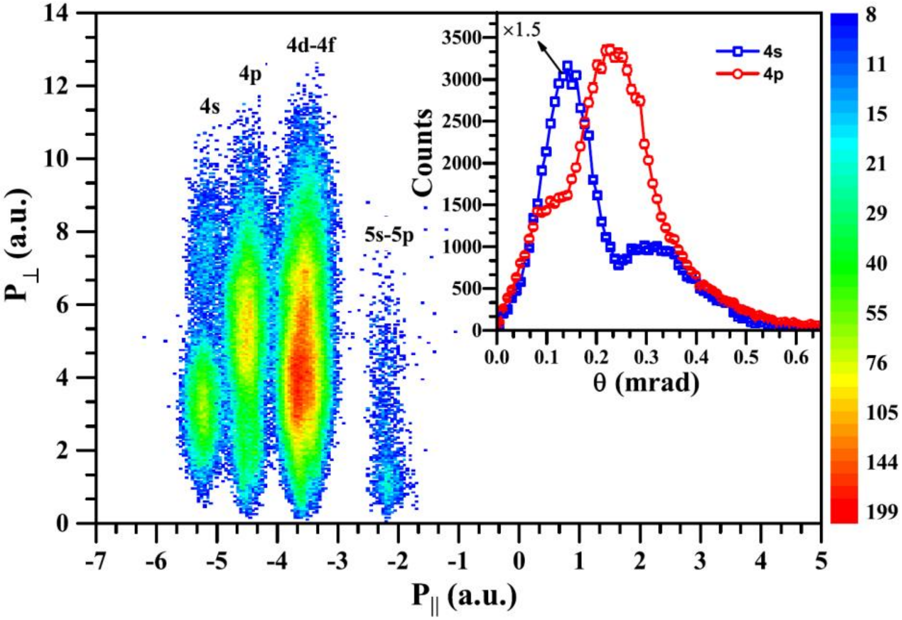

FIG. 2. Two-dimensional momentum distributions in the 3-keV/u Ar^{8+}-He SEC process. The horizontal and the vertical axes represent the longitudinal and the transverse momentum of recoil ions, respectively. In the inset plot, blue squares and red circles represent projectile scattering angle distributions for electron capture into 4*s* and 4*p* states, respectively.

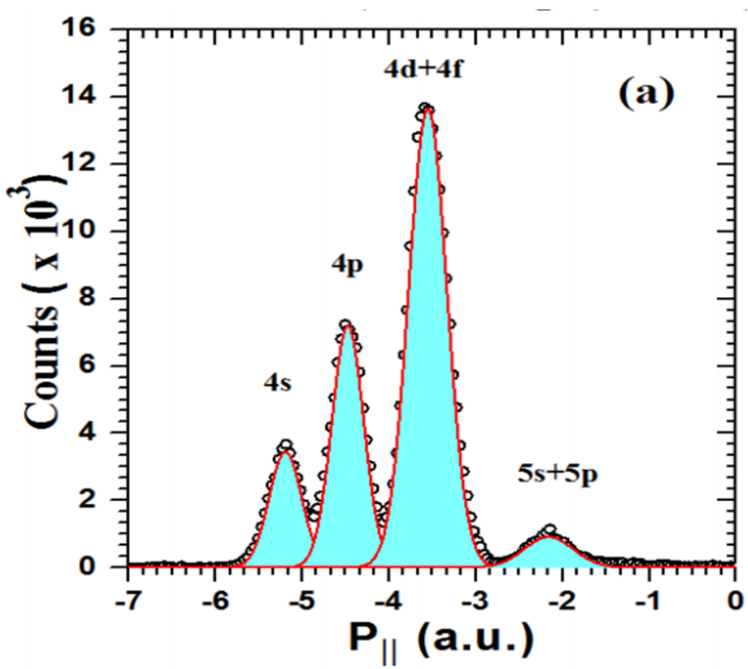

The radial and rotational coupling effects played an important role

R T Zhang et al. Phys. Rev. A 95, 042702 (2017)

State-resolved SEC in Ne^{9+}-He

$Ne^{9+}(1s) + He(1s^2) \rightarrow Ne^{8+}(1snl) + He^{+}$

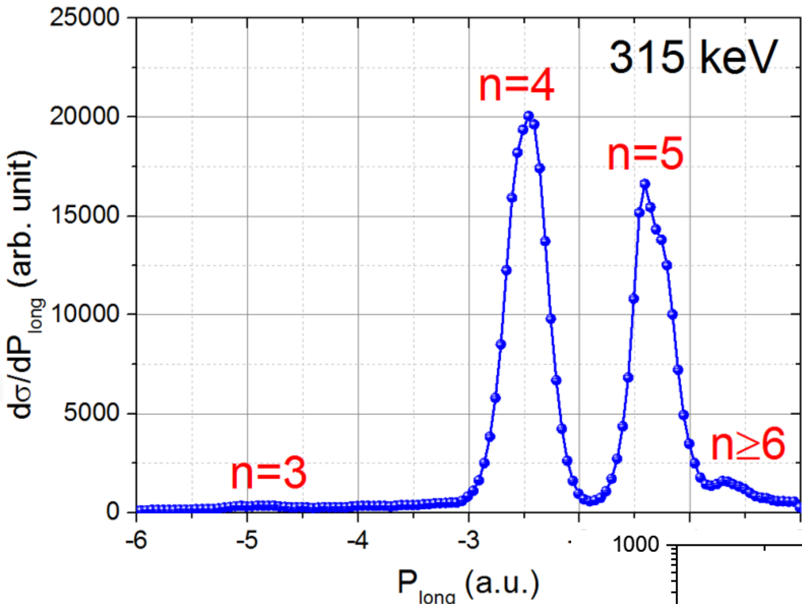

The single electron capture into 4*l* and 5*l* states are dominant. Then contribution of 6*l* states have obvious contribution, while contribution of 3*l* state is rather small.

Relevant to Solar wind processes

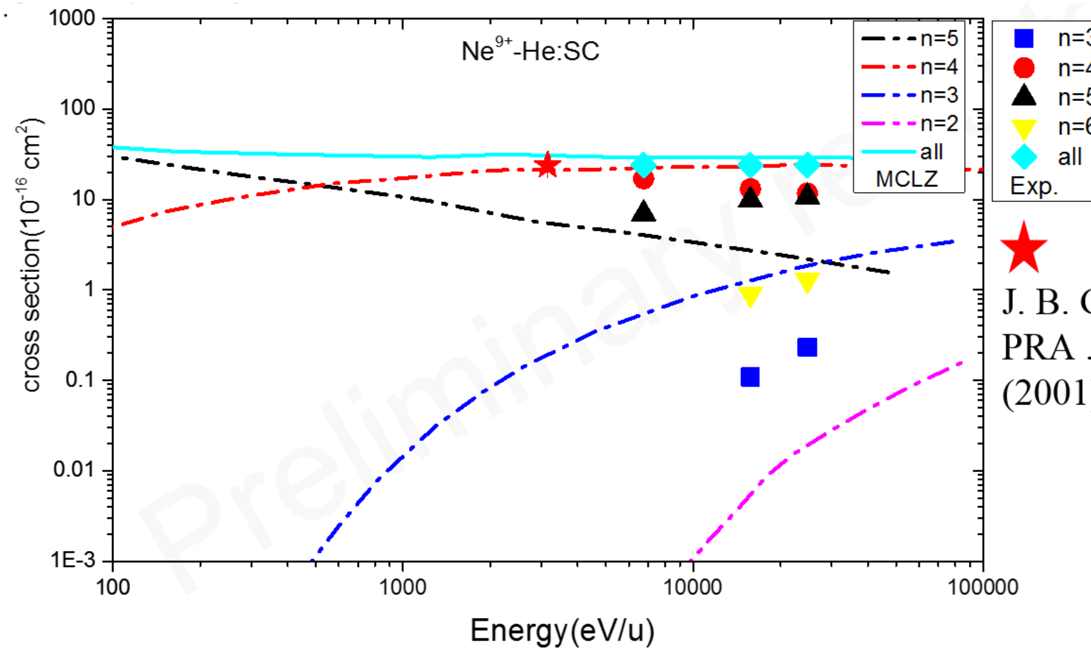

J. B. Greenwood. PRA . 63 062707 (2001)

Phase information of ion-atom collisions

The phase factor in the probability amplitude contains important information of few-body few-body dynamics

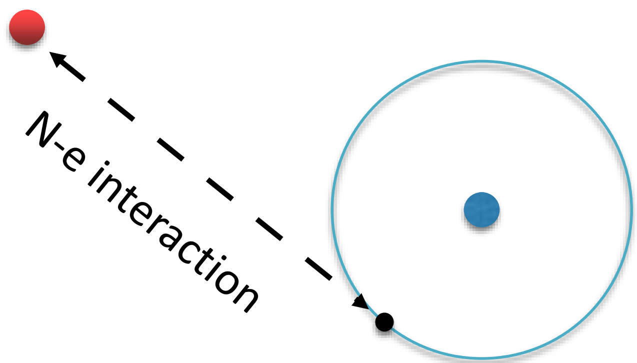

$$A_{Ne} = REAL \times \exp(i\phi)$$

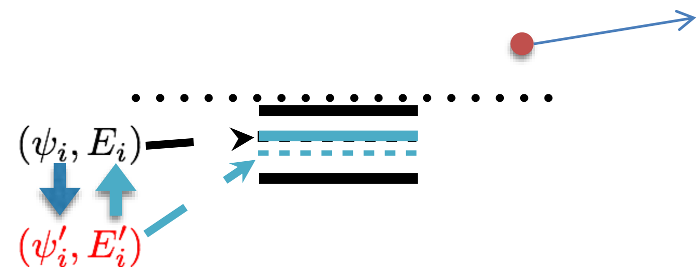

an adiabatic collision process

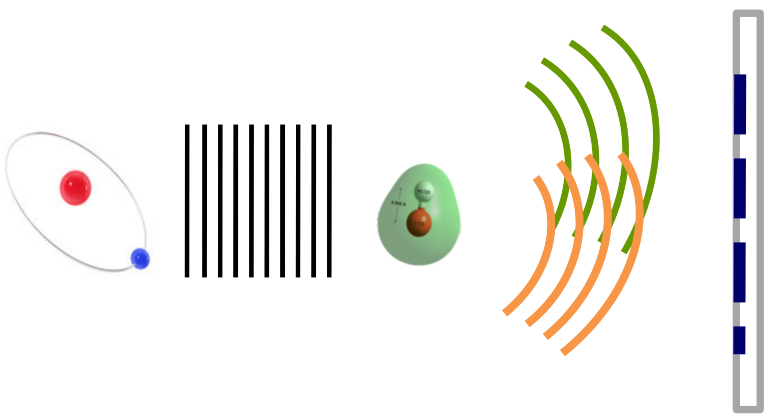

$$\mathrm{He}^{2+} + \mathrm{CO} \rightarrow \mathrm{He} + \mathrm{C}^{+} + \mathrm{O}^{+}$$

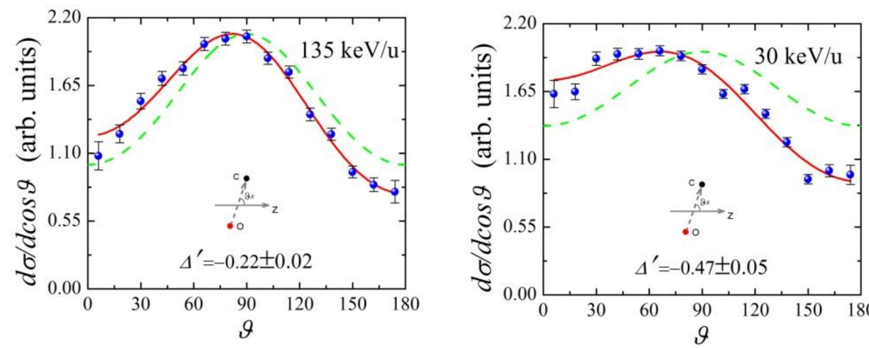

Scattering phase of ion-atom collisions is obtained for the first time

2018 PhysRevA.97.020701(R)

50, 75, 100 keV H^+ - He single capture

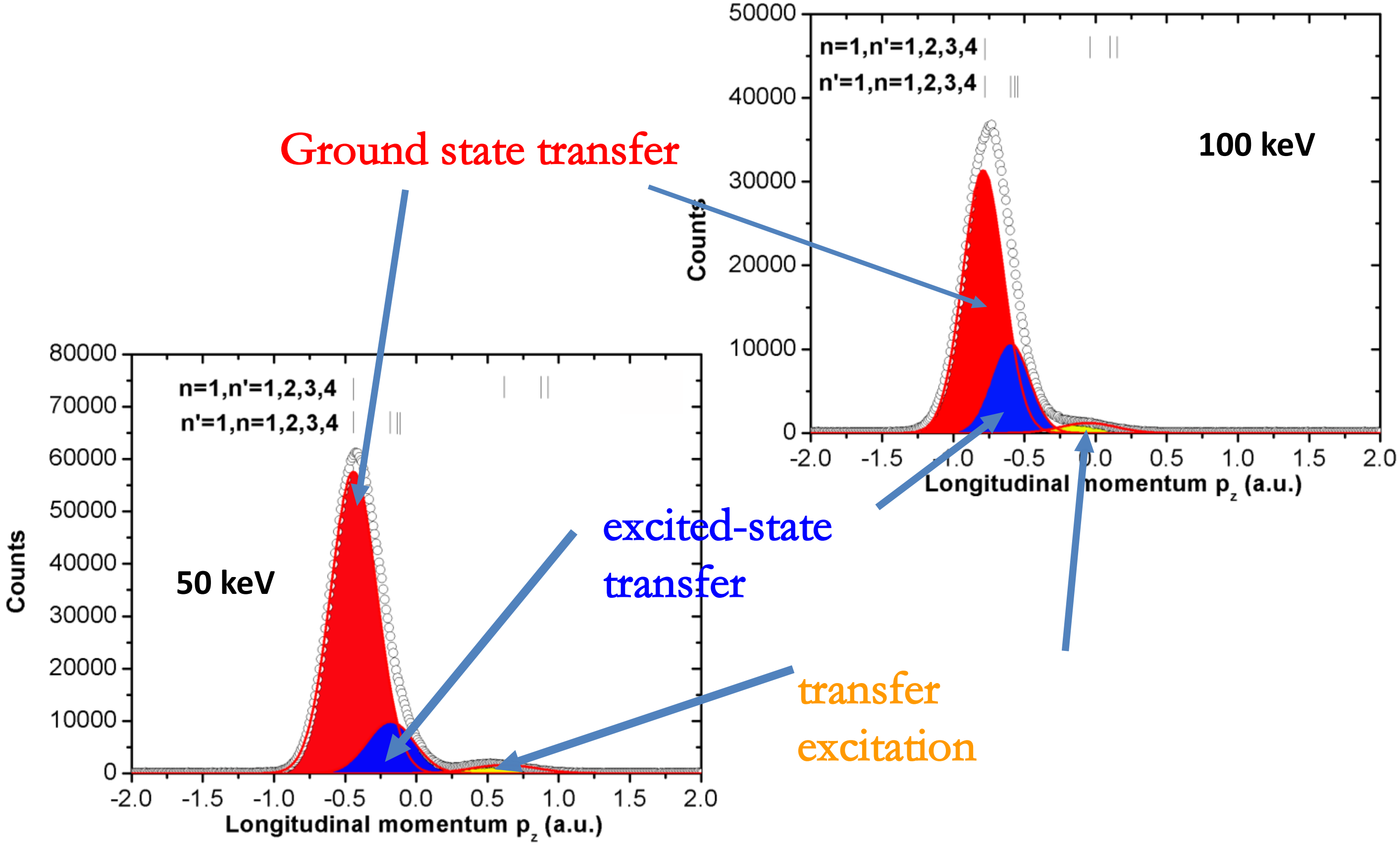

D. L. Guo, X. Ma *et al*, *Phys. Rev. A* 86 052707 (2012)

50, 75, 100 keV H^+ - He single capture

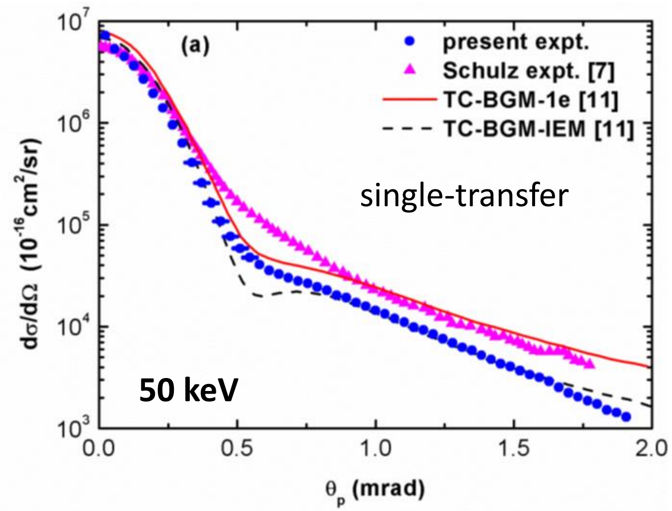

Angular differential cross sections for single-transfer process （50 keV）

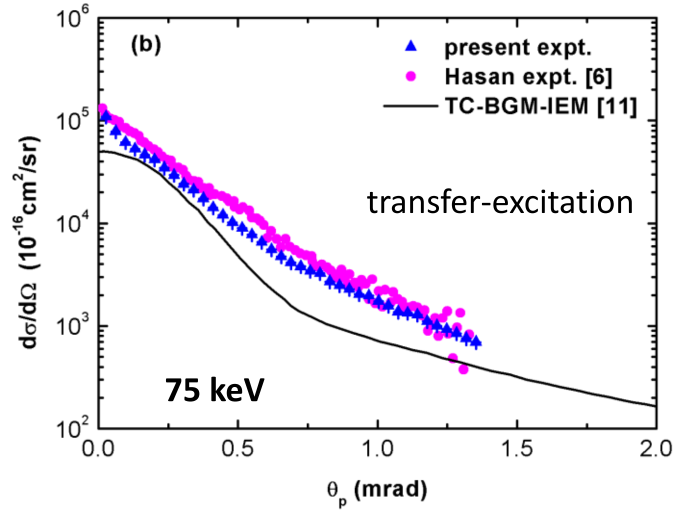

Angular differential cross sections for transfer-excitation process（100 keV）

- **The momentum transfer mediated by the electron is dominant in the single transfer because of the large contributions of small-angle scatterings.**
- **The nucleus-nucleus interaction is more important in transfer excitation.**
- **The electron-electron correlation effects, which can be neglected, may play a role in transfer excitation.**

D. L. Guo, X. Ma *et al*, *Phys. Rev. A* 86 052707 (2012)

50, 75, 100 keV H^+ - He single capture

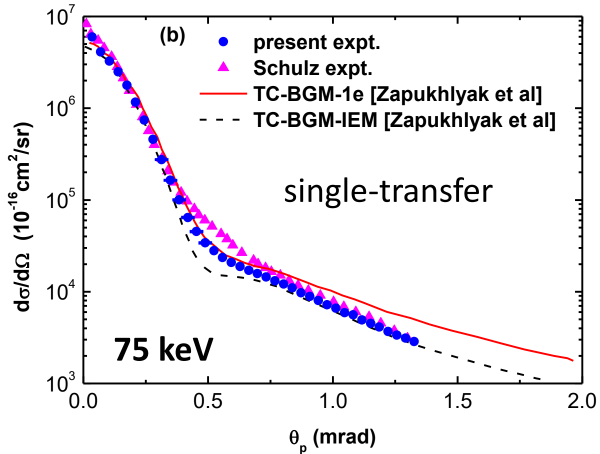

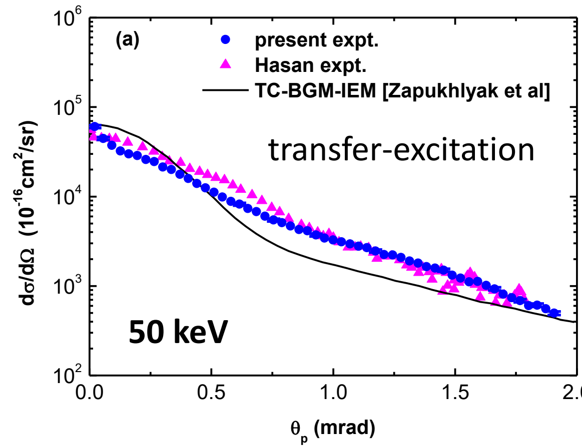

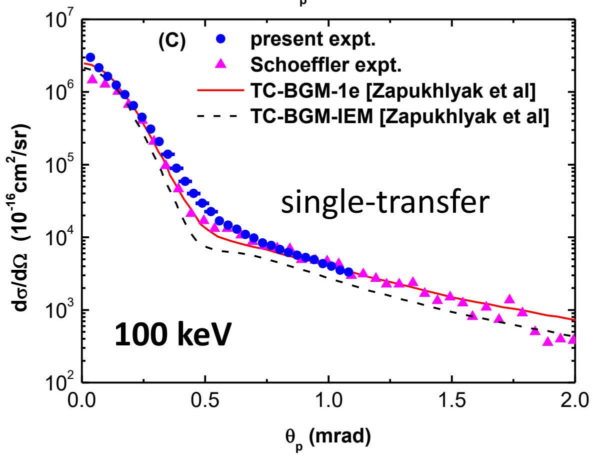

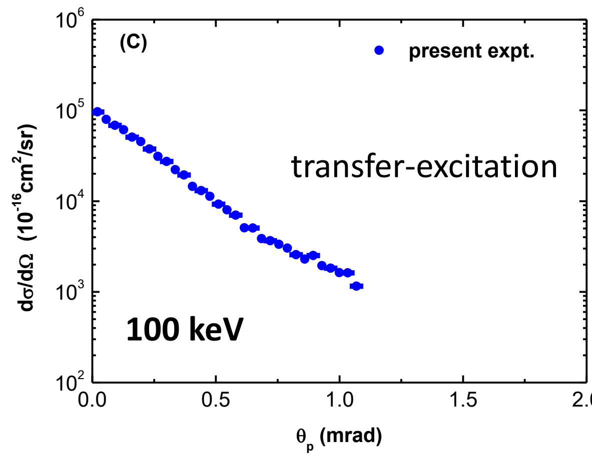

15 , 30, 50 keV/u C^{4+} - He single capture

$$C^{4+}(1s^2)+He(1s^2) \rightarrow C^{3+}(1s^2nl)+He^{+}(n'l')$$

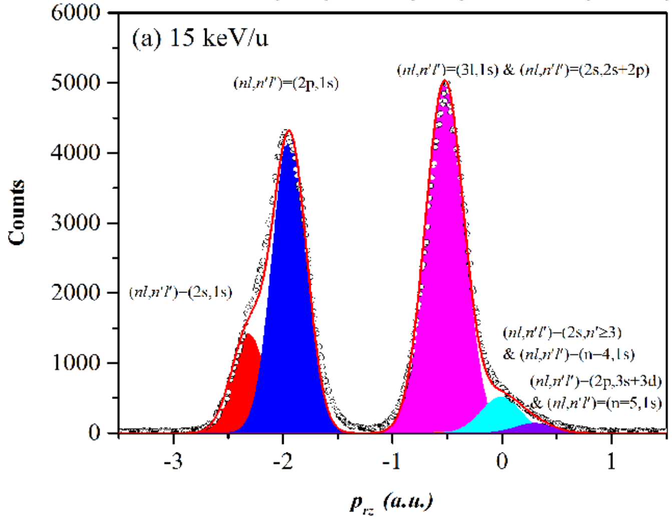

Recoil ion longitudinal momentum

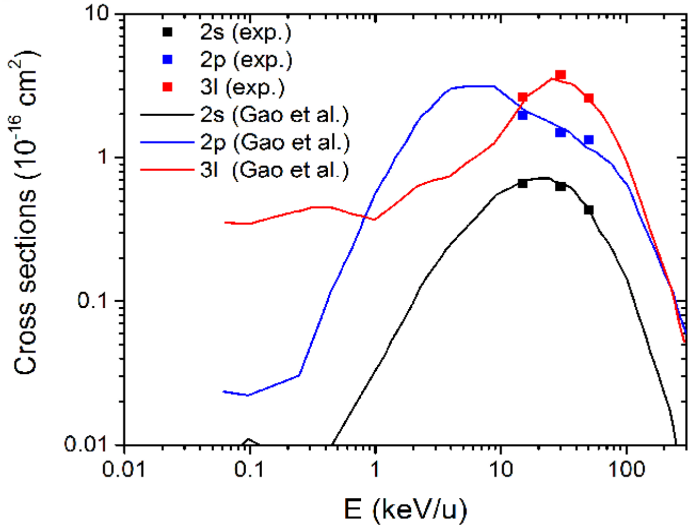

State selective cross sections

Angular differential cross sections (*n=2, n′=1*)

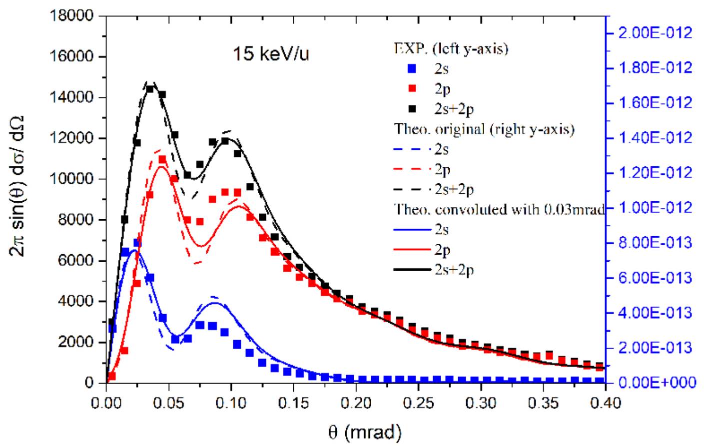

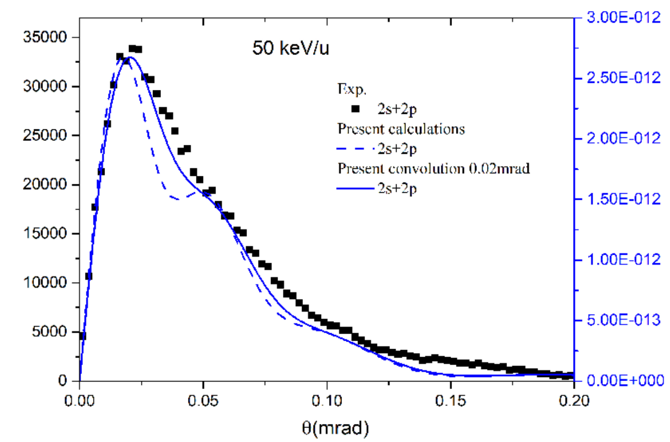

Theory : Two-active electrons AOCC by Gao et al.

State-selective electron capture in N^{3+}-He at 30 keV

$$N^{3+} + He \rightarrow N^{2+}(nl) + He^{+}(n'l')$$

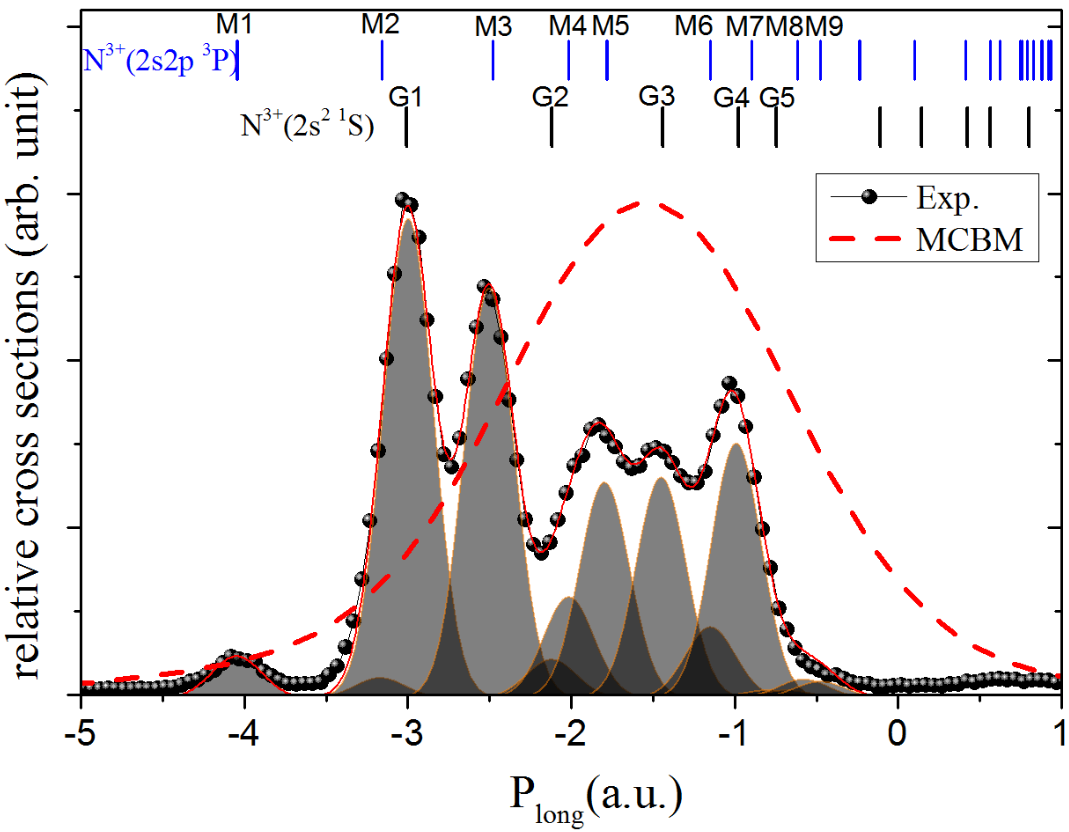

Terms	Initial state	Final states	Q (eV)
G1	$N^{3+}(2s^2\ ^1S)$ +He(^1S)	$N^{2+}(2s^22p\ ^2P)$ +He$^+$(^2S)	22.8
G2		$N^{2+}(2s2p^2\ ^4P)$ +He$^+$(^2S)	15.7
G3		$N^{2+}(2s2p^2\ ^2D)$ +He$^+$(^2S)	10.3
G4		$N^{2+}(2s2p^2\ ^2S)$ +He$^+$(^2S)	6.6
G5		$N^{2+}(2s2p^2\ ^2P)$ +He$^+$(^2S)	4.7
M1	$N^{3+}(2s2p\ ^3P)$ +He(^1S)	$N^{2+}(2s^22p\ ^2P)$ +He$^+$(^2S)	31.2
M2		$N^{2+}(2s2p^2\ ^4P)$ +He$^+$(^2S)	24.1
M3		$N^{2+}(2s2p^2\ ^2D)$ +He$^+$(^2S)	18.7
M4		$N^{2+}(2s2p^2\ ^2S)$ +He$^+$(^2S)	14.9
M5		$N^{2+}(2s2p^2\ ^2P)$ +He$^+$(^2S)	13.1
M6		$N^{2+}(2p^3\ ^4S)$ +He$^+$(^2S)	8.0
M7		$N^{2+}(2p^3\ ^2D)$ +He$^+$(^2S)	6.0
M8		$N^{2+}(2p^2(^1S)3s\ ^2S)$ +He$^+$(^2S)	3.7
M9		$N^{2+}(2p^3\ ^2P)$ +He$^+$(^2S)	2.6

dominant channel G1: $N^{3+}(2s^2\ ^1S)$ +He(^1S) → $N^{2+}(2s^22p\ ^2P)$ +He$^+$(^2S)

M3, M4, M5, G3 and G4 have a significant contribution

the contribution of other states is rather small.

A Niehaus, J. Phys. B: At. Mol. Opt. Phys. 19 2925 (1986). HCI 2018 proceedings

Dissociation of $[HCCH]^{2+}$ to H_2^+ and C_2^+

a benchmark reaction involving
H migration, H–H combination, and C–H bond cleavage

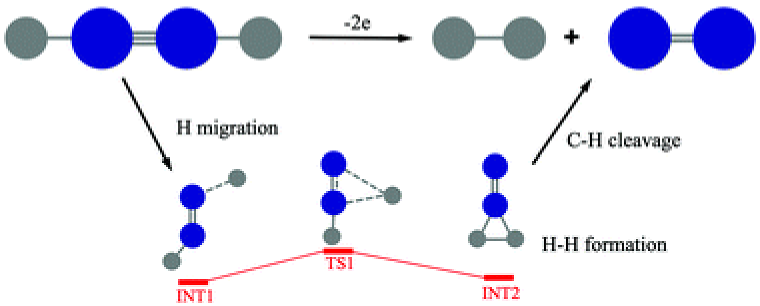

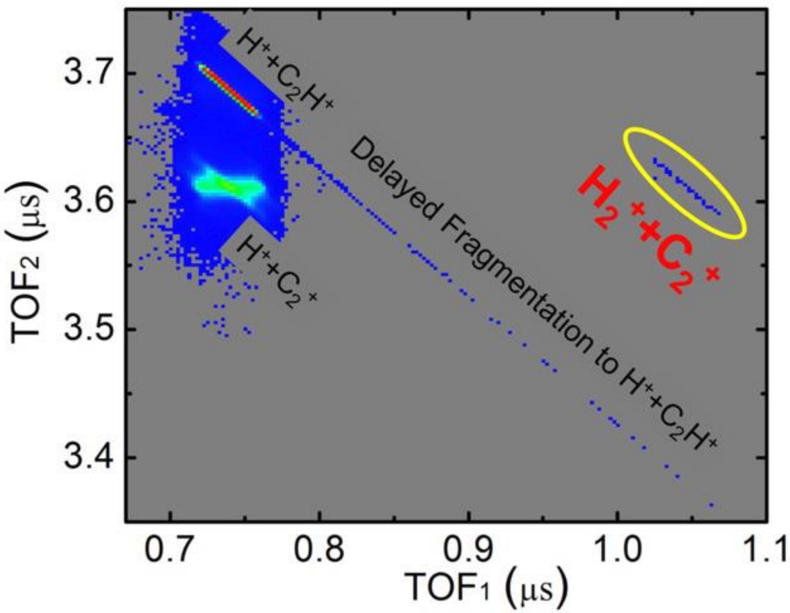

$[HCCH]^{2+}$

dissociates into

$H_2^+ + [CC]^{2+}$

$H^+ + [CCH]^+$

$H^+ + [CC]^+ + H$

Phys.Chem.Chem.Phys.,2018, 20, 27725， DOI: 10.1039/c8cp05780j

p-transfer dissociation in organic molecular dimer: C_2H_2-C_2H_2

Damaging Intermolecular Energy and Proton Transfer Processes in He^{2+} -Irradiated Hydrogen-Bonded Systems

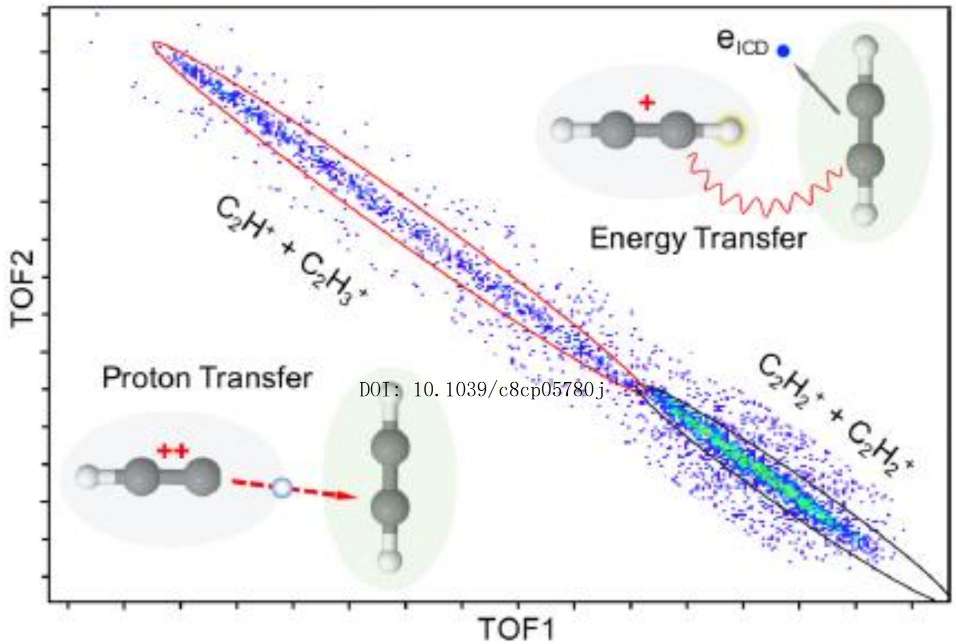

Alpha-particle radiation efficiently damages biologically relevant systems by initiating various intermolecular proton and energy transfer processes.

Angewandte Chemie international addition
https://doi.org/10.1002/anie.201808898

Experiments of HCIs @ Lanzhou

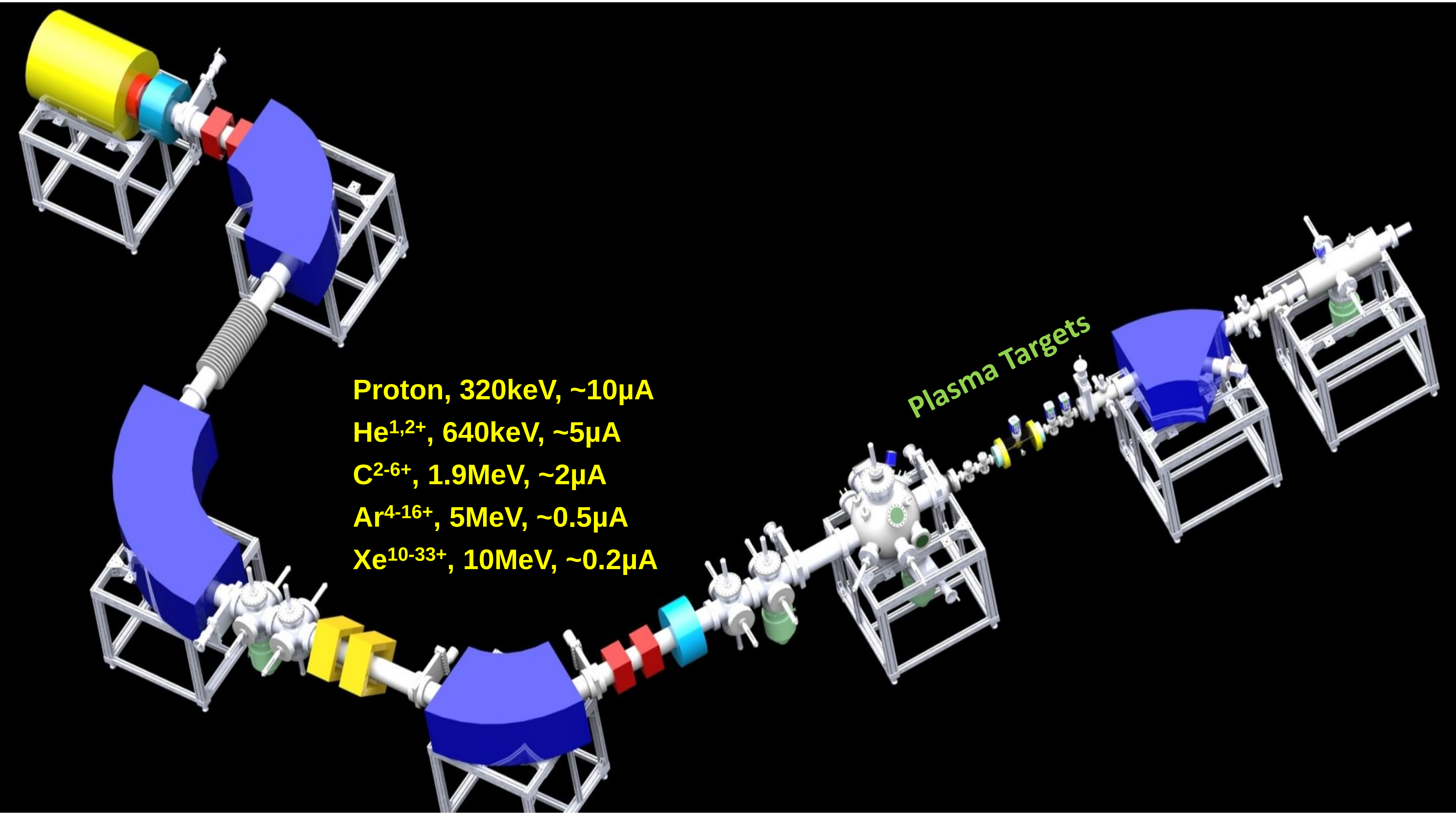

Energy loss in Ion-Plasma Interaction

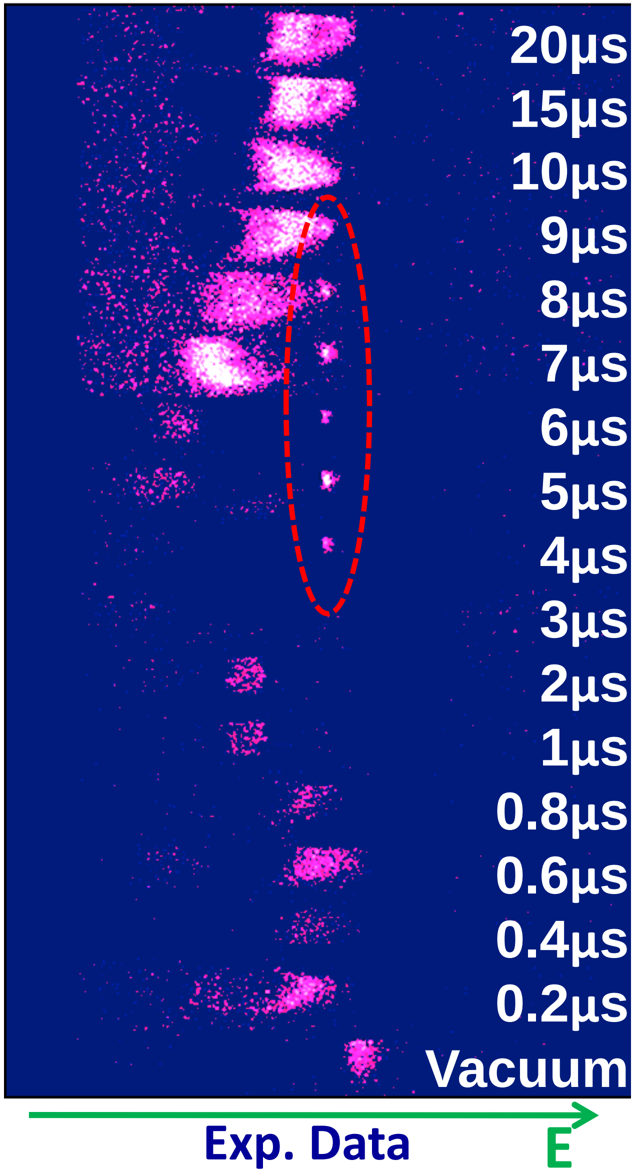

E_0=100keV, P_0=3mbar,HV=3kV

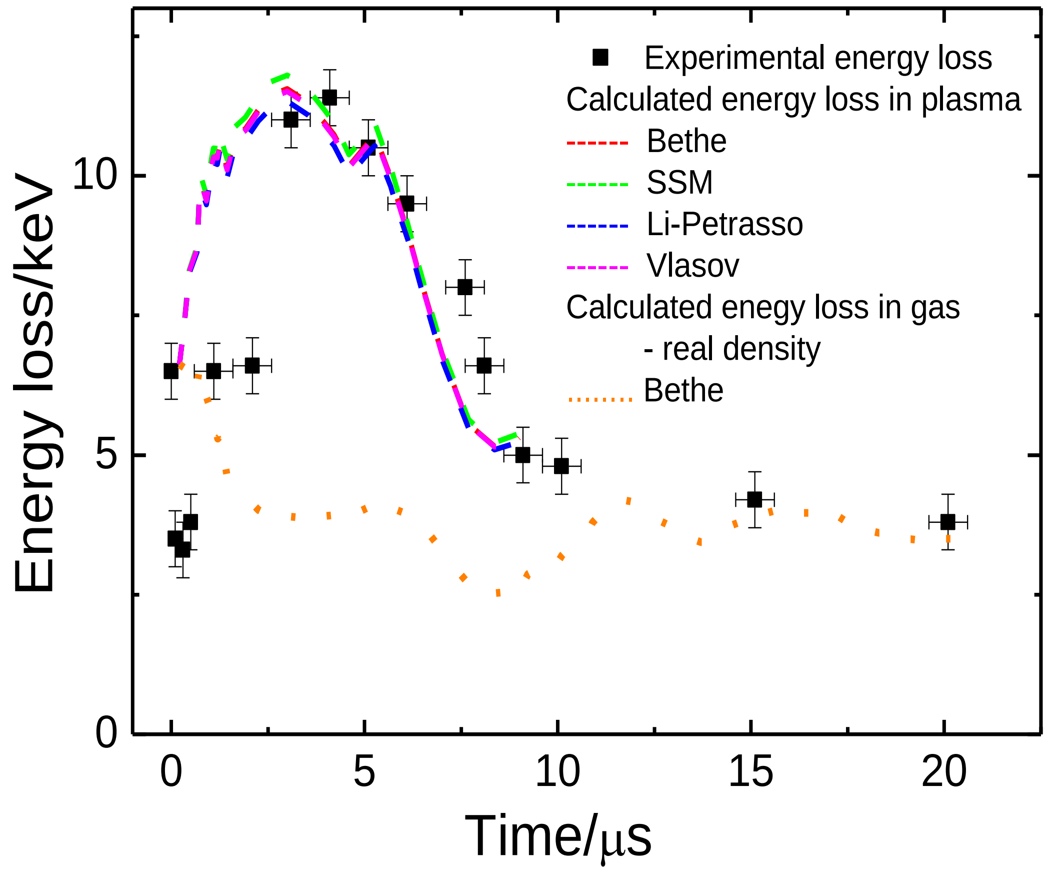

Enhancement of E loss in plasma by a factor of ~3

2. Some typical results related to the atomic data for fusion research and astrophysics

2.2 Precision Spectroscopy of HCIs

Dielectronic Recombination experiment at CSRm

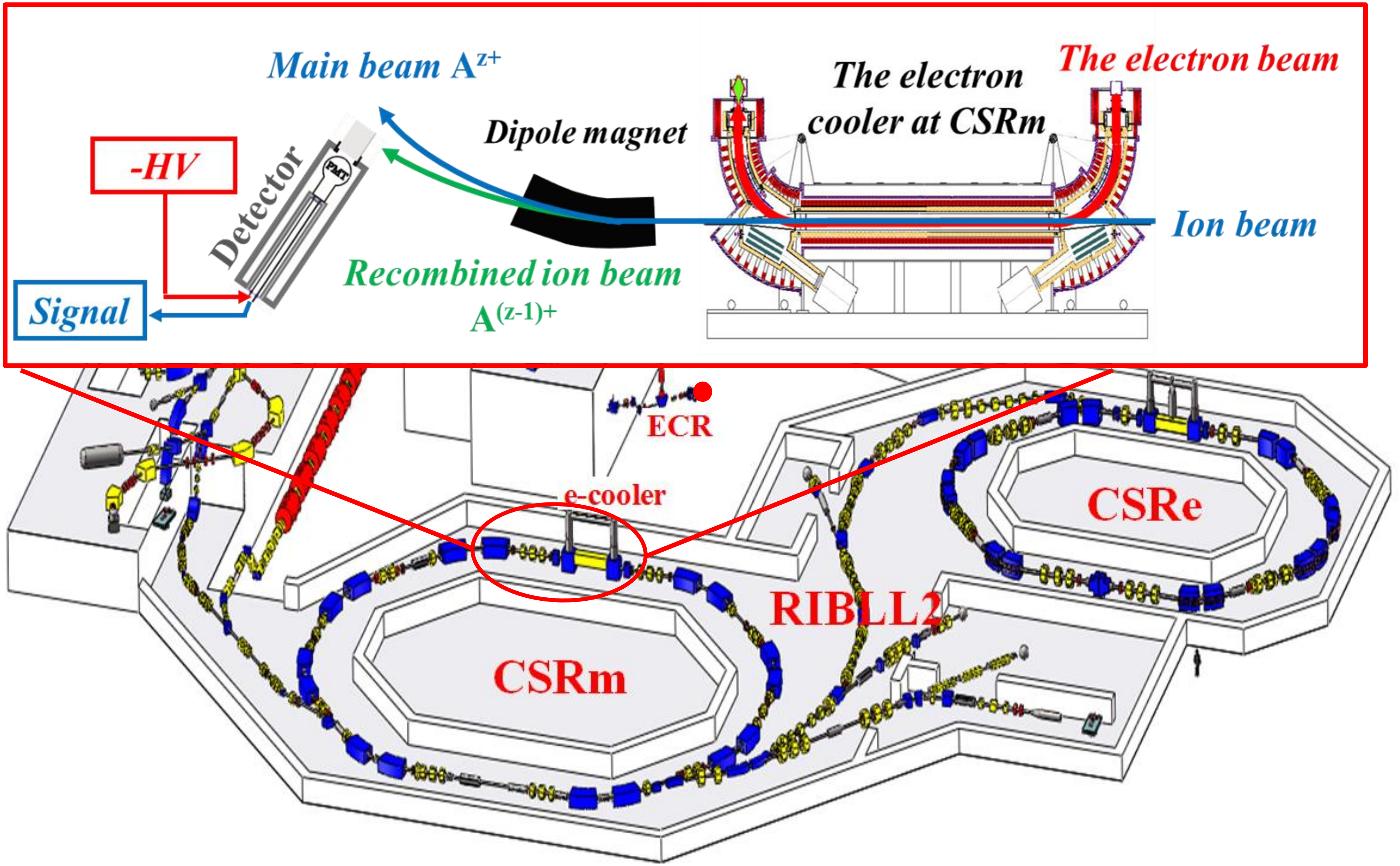

Dielectronic Recombination experiment at CSRm

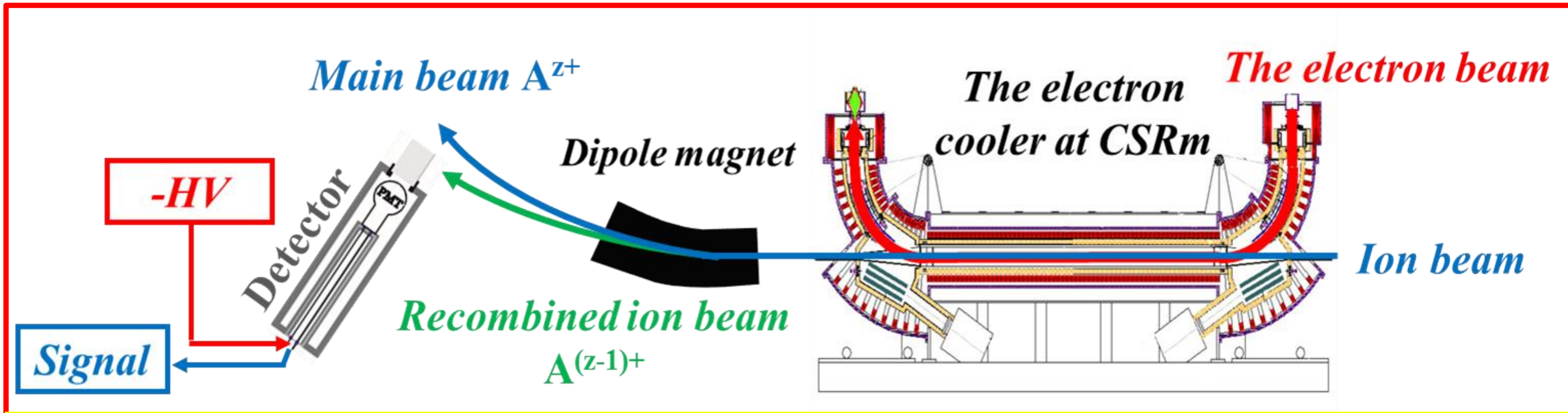

Advantages of DR experiments at heavy ion storage rings

- ultra-high precision (meV， even sub-meV)
- relative energy can be tuned precisely (meV ~ keV)
- recombined ions can be fully detected (100%)
- ultra-high vacuum, extremely low background
- absolute reaction rate can be measured

Results of Li-like argon ions experiment

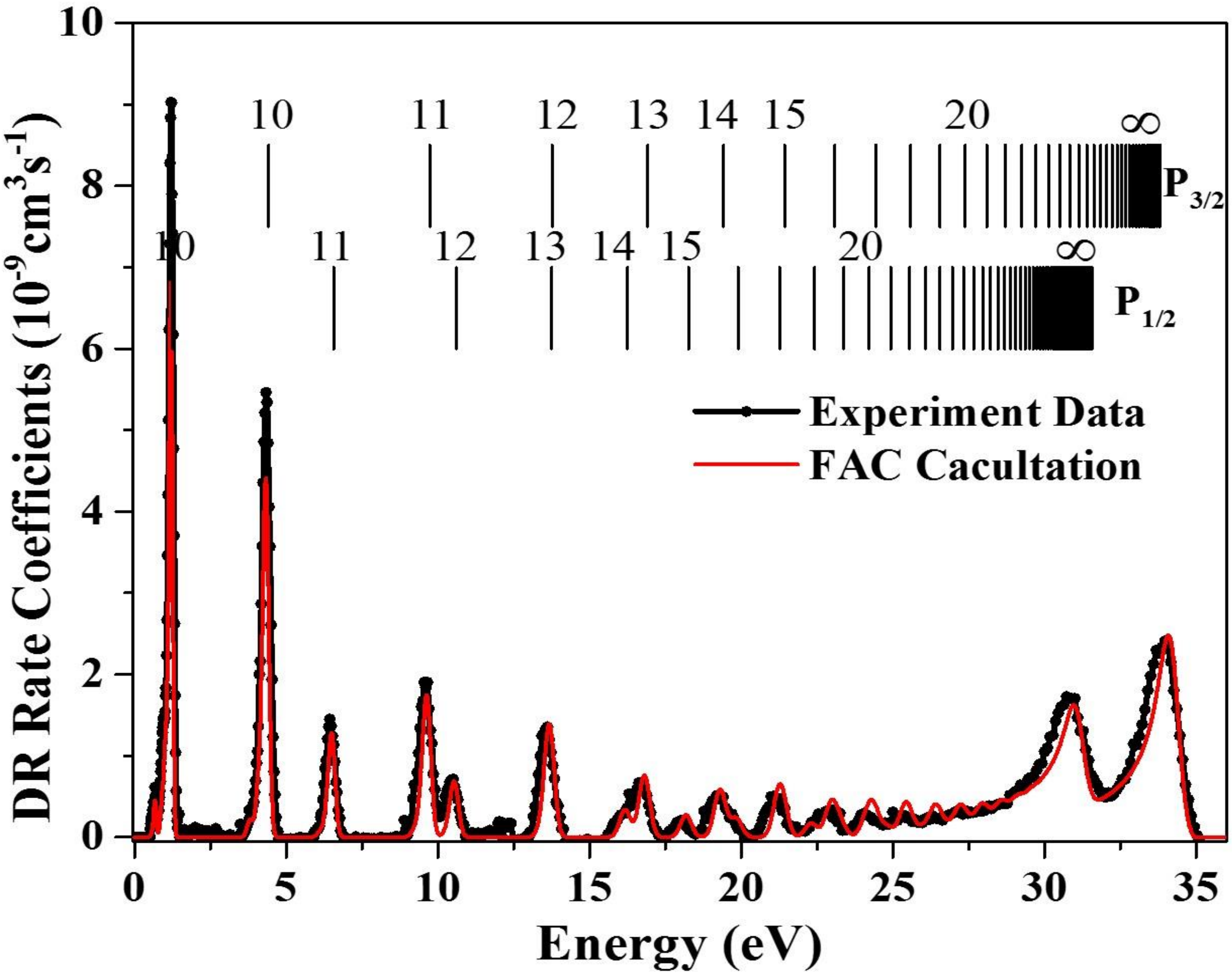

Dielectronic Recombination of Be-like $^{40}Ar^{14+}$ at CSRm

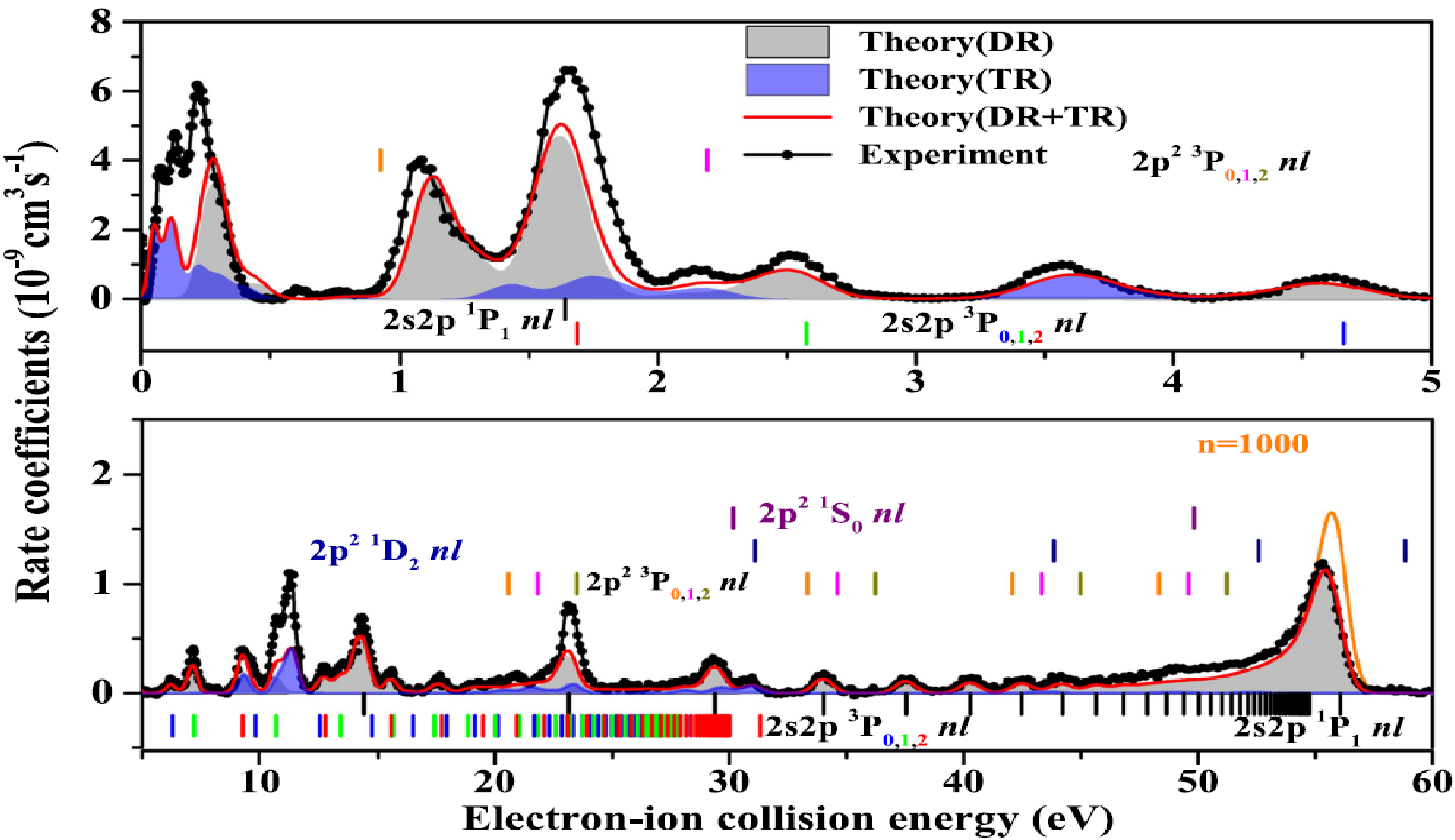

Huang, et al., The Astrophysical Journal Supplement Series 235.1 (2018): 2

Dielectronic Recombination of Be-like $^{40}Ar^{14+}$ at CSRm

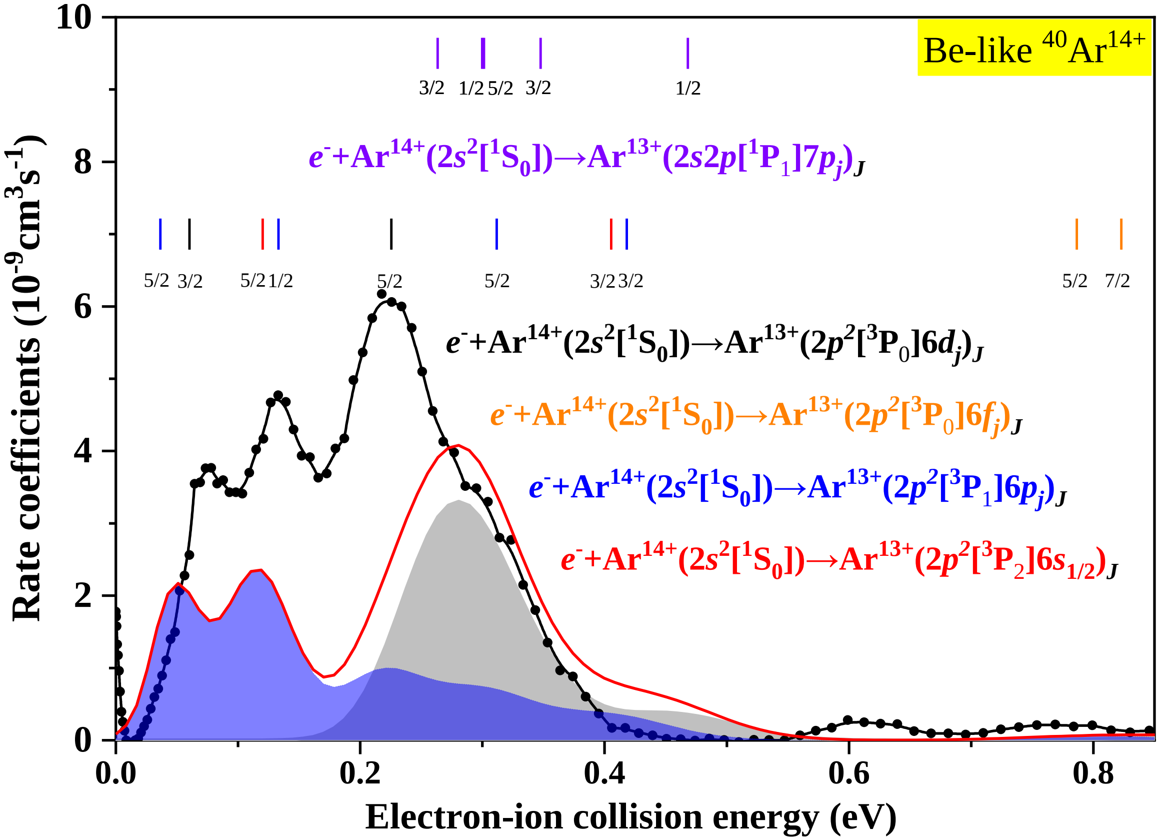

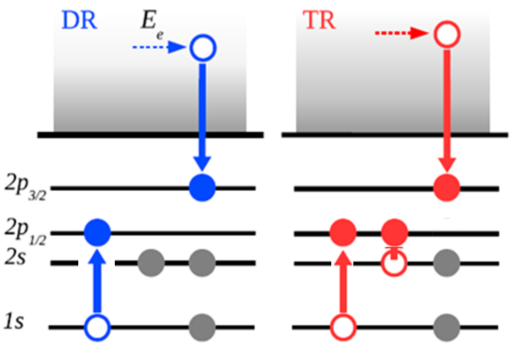

Huang, et al., The Astrophysical Journal Supplement Series 235.1 (2018): 2

Dielectronic Recombination of Be-like $^{40}Ar^{14+}$ at CSRm

Plasma rate coefficients $\alpha(T_e) = \int \alpha(E) f(E, T_e)\, dE$

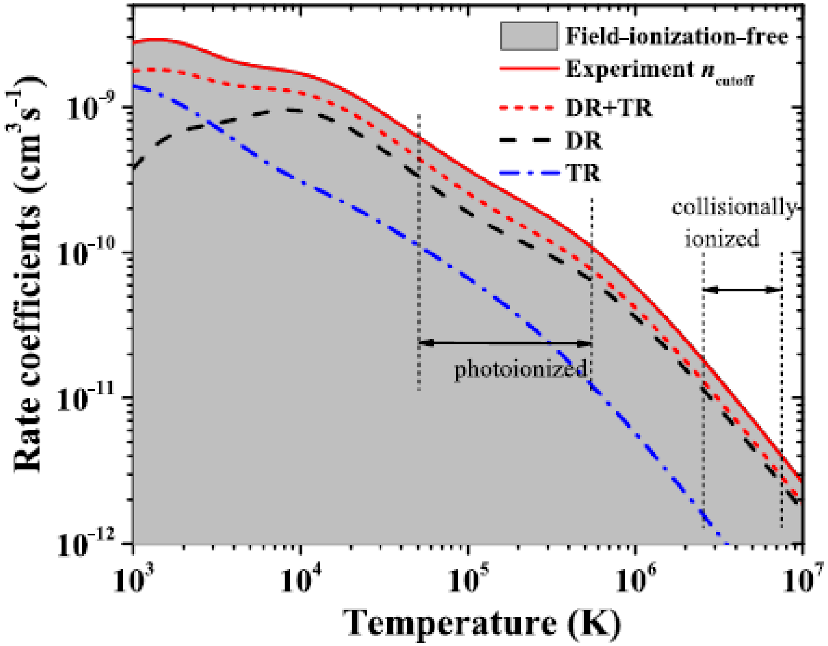

Figure 3. Plasma rate coefficients of Be-like Ar^{14+} as a function of the electron temperature. The solid red line is the experimentally derived $\Delta N = 0$ DR and TR rate coefficients. The theoretical results deduced from the AUTOSTRUCTURE code for $\Delta N = 0$ DR and for TR are shown as a dotted black line and a dashed–dotted blue line, respectively. The calculated sum of DR and TR is shown as a short-dashed red line. The experimentally derived field-ionization-free plasma rate coefficient is shown as a gray area. The approximate temperature ranges where Ar^{14+} is expected to form in photoionized plasmas and collisionally ionized plasmas are indicated by vertical dashed bars and associated arrows (Kallman & Bautista 2001; Bryans et al. 2009).

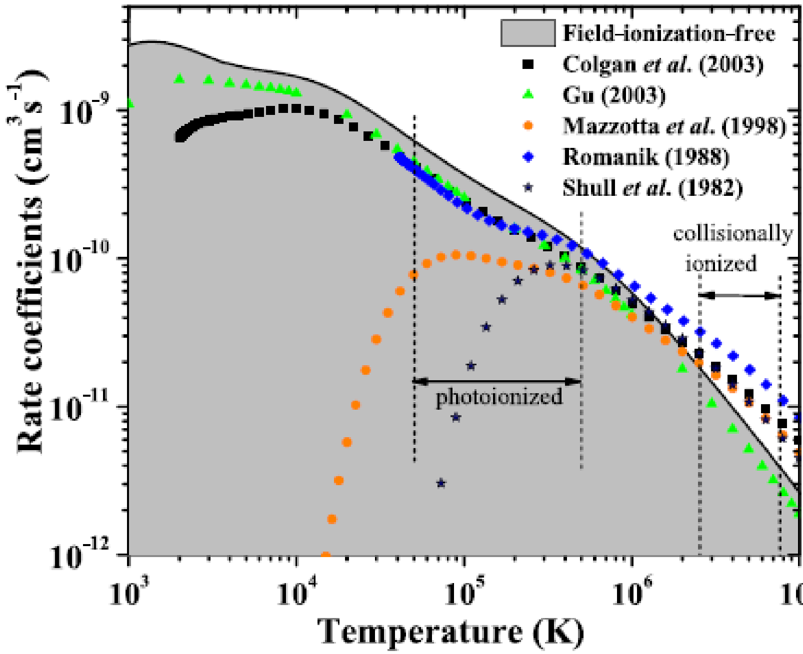

Figure 4. Comparison of field-ionization-free resonant plasma recombination rate coefficients with theoretical calculated results for Be-like Ar. Full squares show rate coefficients by Colgan et al. (2003). Calculations by Gu (2003) and Mazzotta et al. (1998) are shown by full triangles and full circles, respectively. Rate coefficients of Romanik (1988) and Shull & Van Steenberg (1982) are shown by full diamonds and stars, respectively. Temperature ranges where the Be-like Ar concentration is higher than 10% of its maximum abundance in photoionized and collisionally ionized plasmas are shown by vertical dashed bars, as in Figure 3 (Kallman & Bautista 2001; Bryans et al. 2009).

TR has important contr. At low electron tem.

Huang, et al., The Astrophysical Journal Supplement Series 235.1 (2018): 2

Dielectronic Recombination of Be-like $^{40}Ca^{16+}$

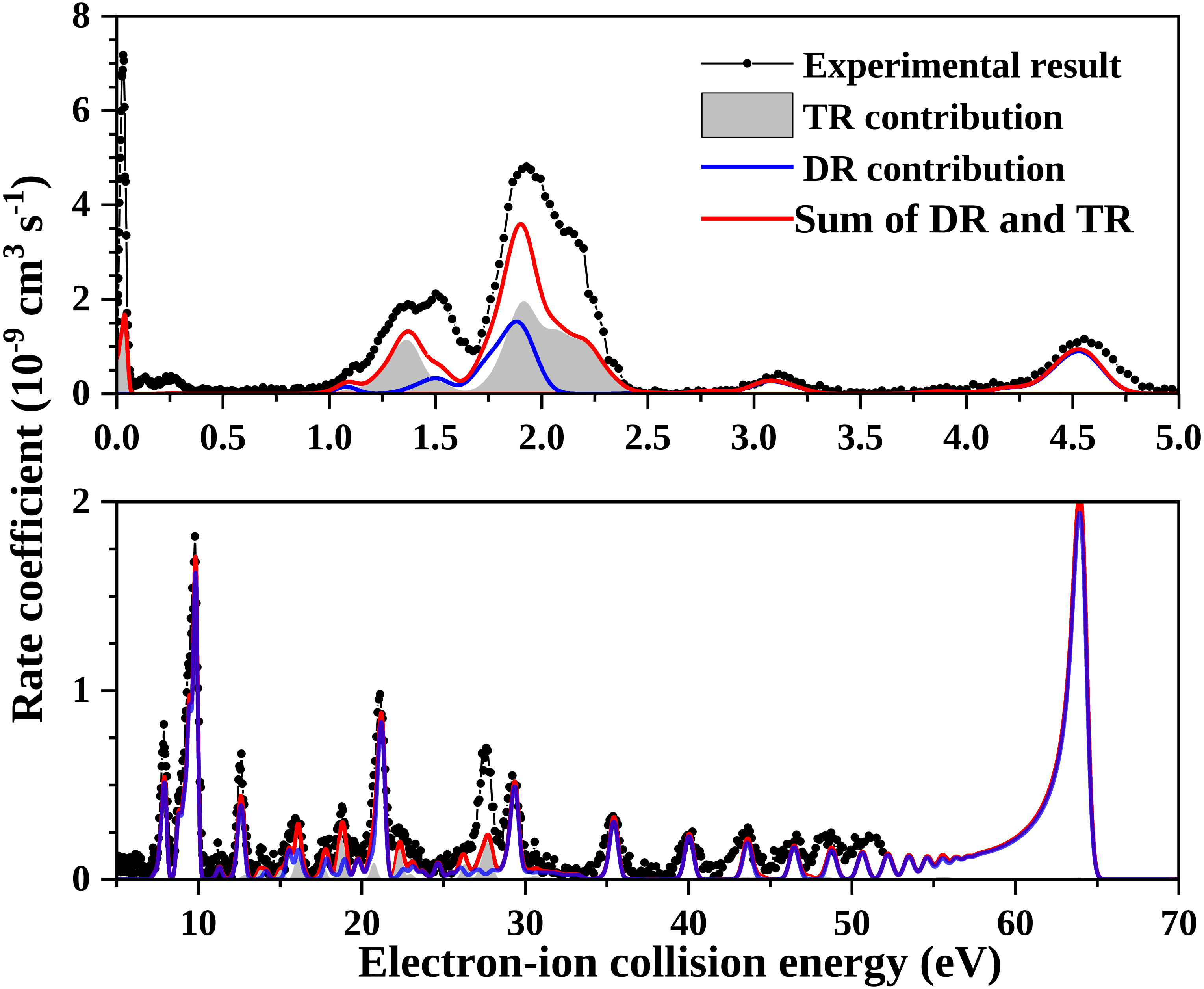

Dielectronic Recombination of Be-like $^{40}Ca^{16+}$

- DR in reasonable agreement with theoretical results
- TR obvious disagreements with theoretical results
- Metastable states contribute to DR at low energy

$$e^- + Ca^{16+}\left(1s^2 2s^2[^1S_0]\right) \rightarrow Ca^{15+}\left(1s^2 2p^2[^1D_2]6l_j\right)_J^{**}$$

$$e^- + Ca^{16+}\left(1s^2 2s^2[^1S_0]\right) \rightarrow Ca^{15+}\left(1s^2 2s2p[^3P_2]10l_j\right)_J^{**}$$

$$e^- + Ca^{16+}\left(1s^2 2s2p[^3P_0]\right) \rightarrow Ca^{15+}\left(1s^2 2p^2[^3P_1]8l_j\right)_J^{**}$$

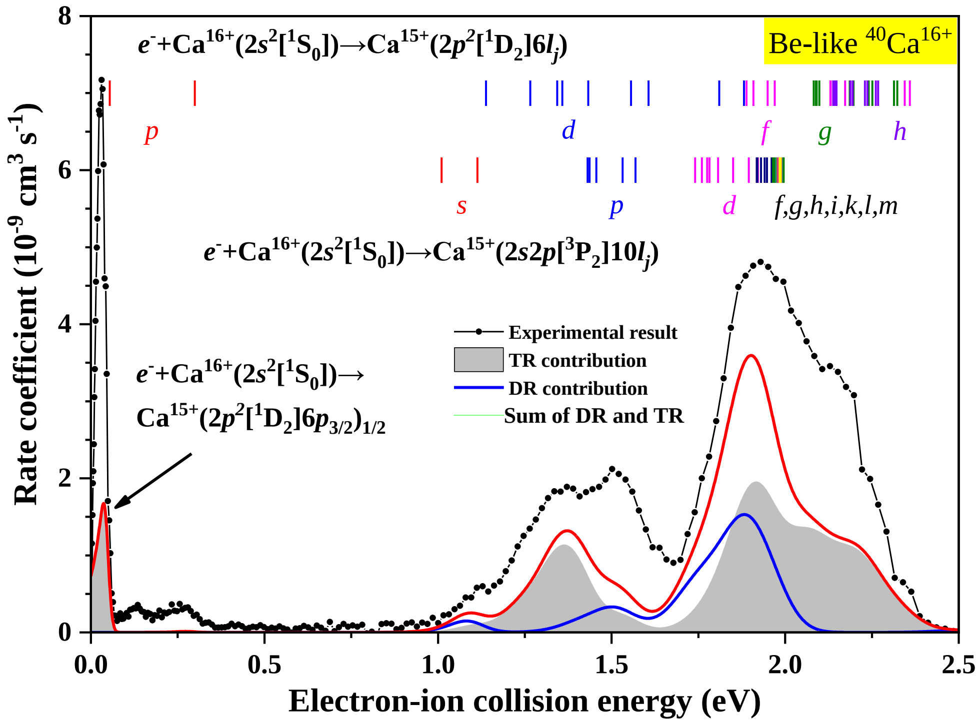

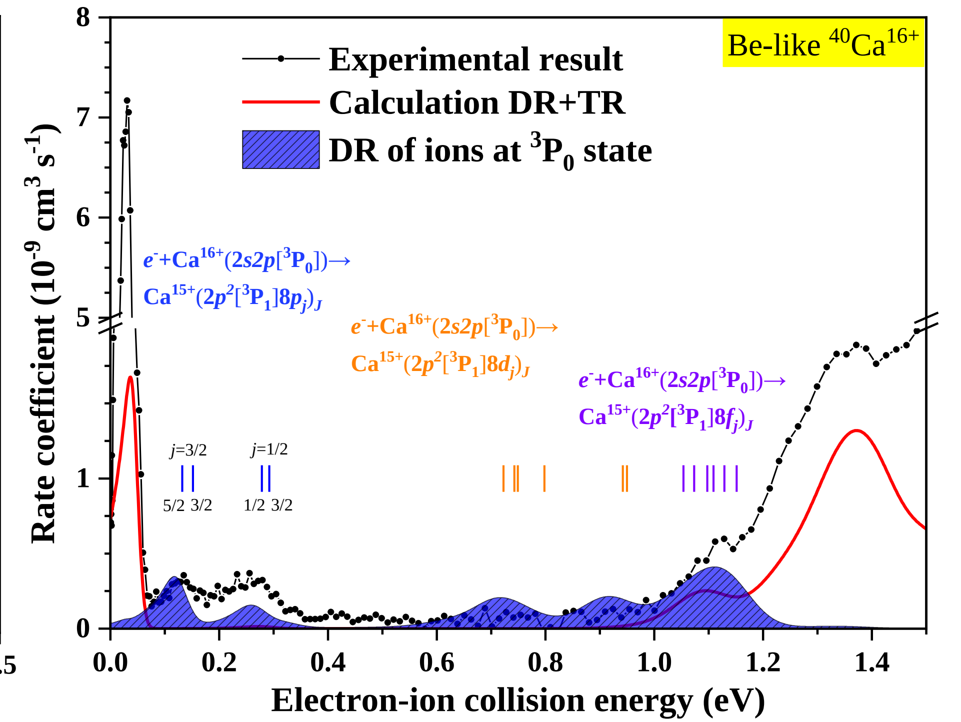

Dielectronic Recombination of Be-like $^{40}Ca^{16+}$

$$\alpha(T_e) = \int \alpha(E) f(E, T_e)\, dE$$

E-ion recombination rates

$$f(E, T_e) = \frac{2E^{1/2}}{\pi^{1/2}(k_B T_e)^{3/2}} \exp\left(-\frac{E}{k_B T_e}\right)$$

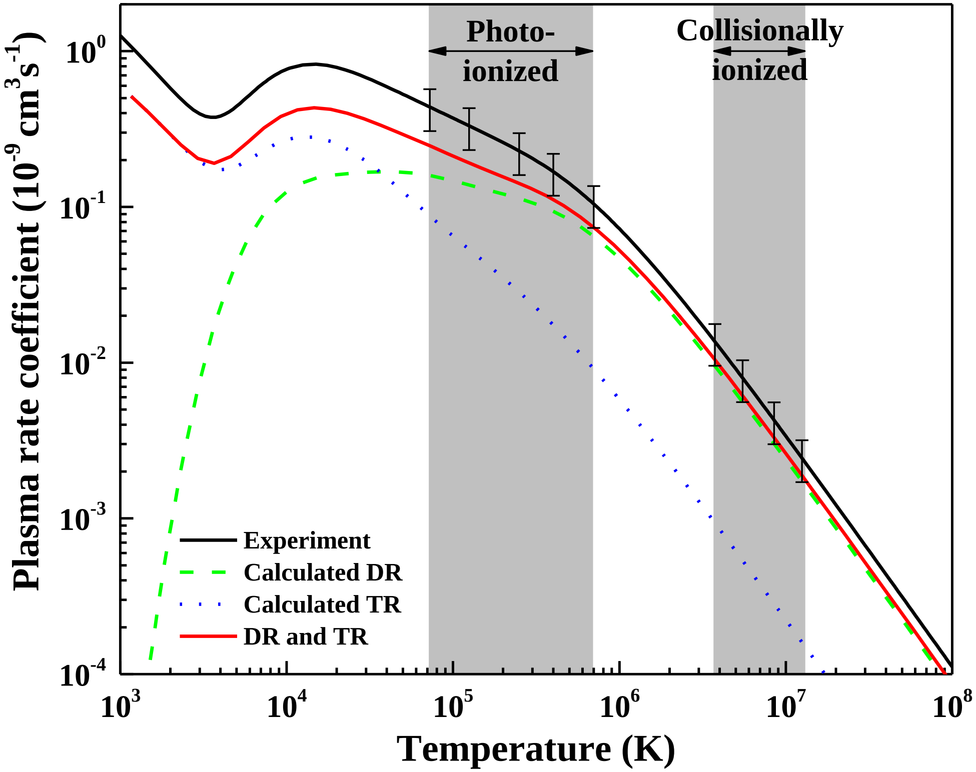

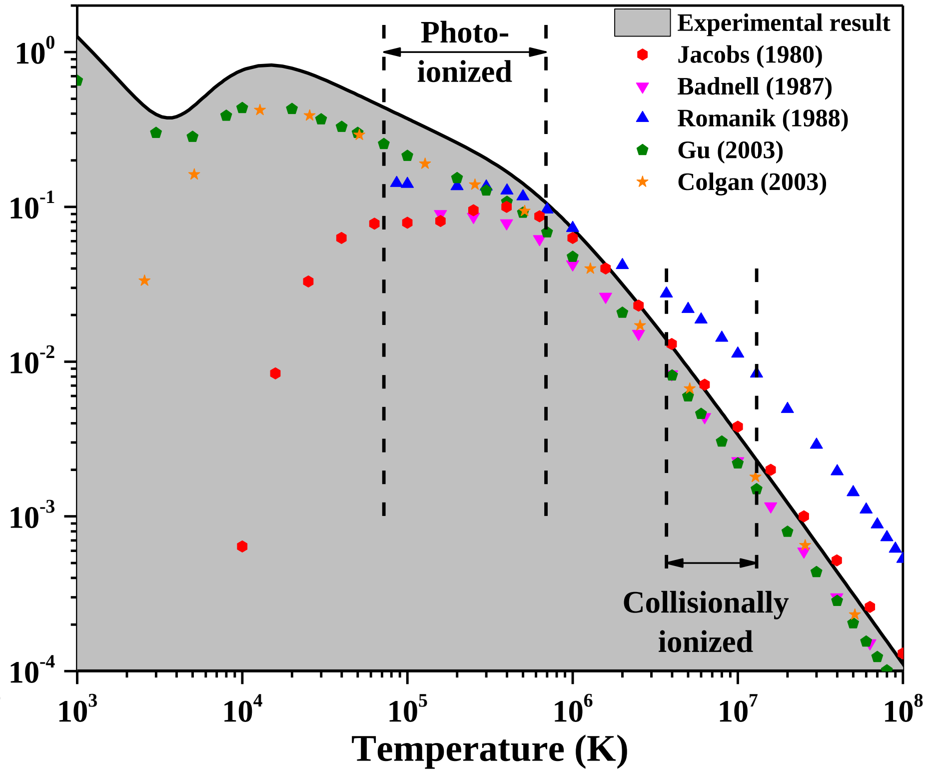

Shu-Xing Wang *et al*. Astrophys. J. 862(2), 134

Experimental results: B-like Ar^{13+}

With upgrade of the HV system, higher resolution, ~0.03 eV

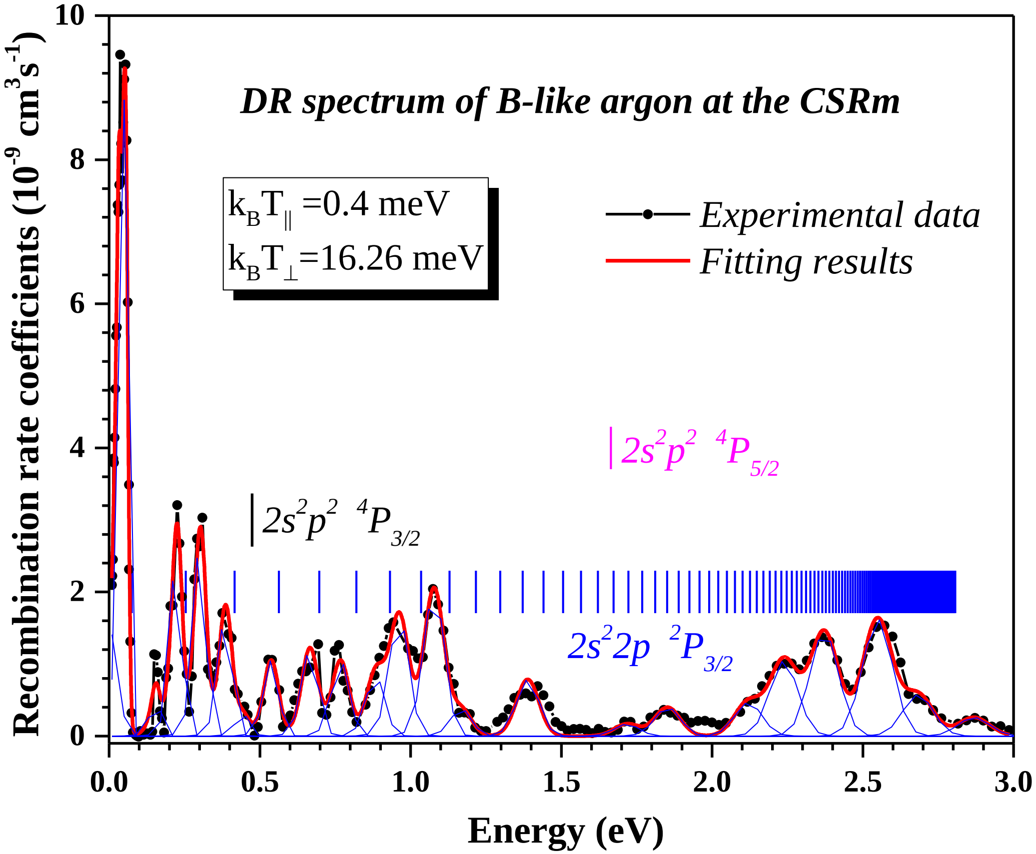

The vertical bar indicated in the figure is estimated by Rydberg formula:

$$E_{res} = E_{exc} - \frac{RZ_{eff}}{n^2}$$

E_{exc} is the core excitation energy
R is the Rydberg constant
Z_{eff} is the charge of the target ion

$$\Delta E = \sqrt{(\ln 2 \cdot k_B T_{\perp})^2 + 16 k_B T_{\parallel} \cdot E_{rel} \cdot \ln 2 + \Gamma^2} + \frac{\Delta p}{p} \cdot (\beta_i - \beta_e)\gamma_i \gamma_e \cdot m_e c^2$$

3. Near future working plans and collective action of data for fusion research and astrophysics

Activities related to atomic data for Fusion and Astrophysics

1. DR rates for W/Au ions
2. Collective action on absolute cross section measurements with higher accuracy for ion-atom/molecules collision, Fudan Univ. + IMP
3. Dynamics of State resolved charge exchange processes
4. Energy loss: keV ion-plasma interaction

Ion-atom/molecule Collision Collaboration

IMPCAS, Lanzhou	X. Ma, S. F. Zhang, X. L. Zhu, S. C. Yan, D. L. Guo, Y. Gao, J. W. Xu, Z. J. Wang, X. X. Wu, M. Zhang, B. Hai, D. P. Dong, Z. T. Lei,
USTC, Hefei	X. J. Chen, X. Shan, X. Zhao, Z. J. Shen, L. Chen, W. Z. Huang
UCAS, Beijing	Y. Z. Qu
IAPCM, Beijing	J. G. Wang, Y. Wu, and L. Liu
Uni. FuDan ShangHai	B. R. Wei, Y. Zhang
MUST, Missouri USA	M. Schulz
HHU Düsseldorf	A. B. Voitkiv

DR Collaboration

IMPCAS, Lanzhou	**X. Ma* , Z.K. Huang, W.Q. Wen, H.B. Wang, S. Mahmood, N. Khan, L.J. Dou, X.L. Zhu, D.M. Zhao, L.J. Mao, J. Li, X.M. Ma, D.Y. Yin, Y.J. Yuan, J.C. Yang;**
USTC, Hefei	**S.X. Wang, X. Xu, W.Q. Xu, L.F. Zhu;**
Uni. Fudan, Shanghai	**T.H. Xu, K. Yao, Y. Yang, C.Y. Chen;**
GSI, Darmstadt	**Th. Stöhlker, C. Brandau, A. Gumberidze, Yu. Litvinov, M. Steck;**
Uni. Giessen	**A. Müller, S. Schippers;**
BINP, Novosibirsk	**V. V. Parkhomchuk, V. B. Reva;**
IAPCM, Beijing	**C.Y. Li, X.Y. Han, J.G. Wang;**
NWNU, Lanzhou	**L.Y. Xie, D.H. Zhang, C.Z. Dong, ;**
Uni. Strathclyde, Glasgow	**N.R. Badnell, Simon Preval;**

特别致谢Acknowledgements：

国家自然科学基金（NSFC)

科技部(MOST)

中国科学院(CAS)

感谢大家的关注

Vielen Dank

Thank you for your attention